Dual space-conjugated pyrene-based ketone exhibits the dual state-tuned emission wavelengths and enhanced circularly polarized luminescence

Yao Ji,[a] Xin Meng,*[a] Jia'ao Han,[a] Yanchen Liu,[a] Jian Tang,[a,b] Yuanchun He,[a] Ensheng Zhang,[a] Xiaoxiang Zhang,[c] Ziping Cao*[a]

[a] Shandong Key Laboratory of Life-Organic Analysis and School of Chemistry and Chemical Engineering, Qufu Normal University, Qufu, 273165, Shandong, P. R. China. E-mail: caozp_qfnu@163.com (ziping@qfnu.edu.cn); mengxin1108@163.com (mengxin@qfnu.edu.cn)

[b] State Key Laboratory of Coordination Chemistry, Nanjing University, Nanjing 210023, P. R. China

[c] College of Chemical Engineering, Nanjing Forestry University, Nanjing 210037, P. R. China

General. All the reactions were carried out under N_2 atmosphere unless otherwise specified. Melting points (m.p.) were measured on an *X-4 microscope* apparatus and are uncorrected. NMR-spectra were measured in the given solvent at RT on *Bruker Avance III HD 500* (500.1 MHz, 1H; 125.8 MHz, 13C) instrument operating at the denoted spectrometer frequency given in mega Hertz (MHz) for the specified nucleus. High-resolution mass spectrometry with electrospray ionization (ESI-HRMS) was recorded on a *Bruke P-SIMS-Gly FT-ICR* mass spectrometer. UV-visible (UV-vis) absorption spectra were recorded on a *UV-3600Plus* spectrometer from Shimadzu. Fluorescence spectra were performed with an *Agilent Cary Eclipse* spectrometer. Relative quantum yields were determined using *fluorescein* as standard. The fluorescence decay curves were obtained using the time-correlated single-photon-counting method on a *FLS1000 Photoluminescence Spectrometer* from Edinburgh Instruments. IR-spectra were obtained on a Thermo Fisher spectrometer at the range of 4000–400 cm^{-1}. PXRD patterns were obtained on a PANalytical X-ray diffractometer model X'pert3 with graphite monochromatized Cu Kα radiation (λ = 0.154 nm) at 2θ ranging from 5 to 50°. The ECD spectra were measured on a *JASCO J-810* circular dichroism spectrometer. CPL spectra were recorded on a *JASCO CPL-300* spectrometer. Particle size distributions were evaluated using the dynamic light scattering (DLS) method on a *Malvern Zetasizer Nano ZS* system.

All the density functional theory (DFT) and time-dependent DFT (TD-DFT) calculations were carried out using *Gaussian 16*, *Revision C.01*.[1] The PBE0 functional in combination with 6-31G(d,p) basis set and GD3 empirical dispersion correction were used for

optimization, single point energy, vertical excitation energy and excited-state geometry optimization. The single crystal structures were used as the initial structures for DFT optimization and then other calculations. To make that the optimized geometry represented a minimum, each geometry optimization (S0 and S1) was followed by a frequency calculation, yielding only positive frequencies. Intermolecular interactions were theoretically evaluated by the Hirshfeld surfaces (mapped over *d*_norm) and decomposed fingerprint plots.[2] Weak interaction analysis was performed based on the IRI method.[3] All the calculated results were analyzed and drawn by the *GaussView 6.0* or *Multiwfn_3.8_dev or VMD 1.9.3* program.[4]

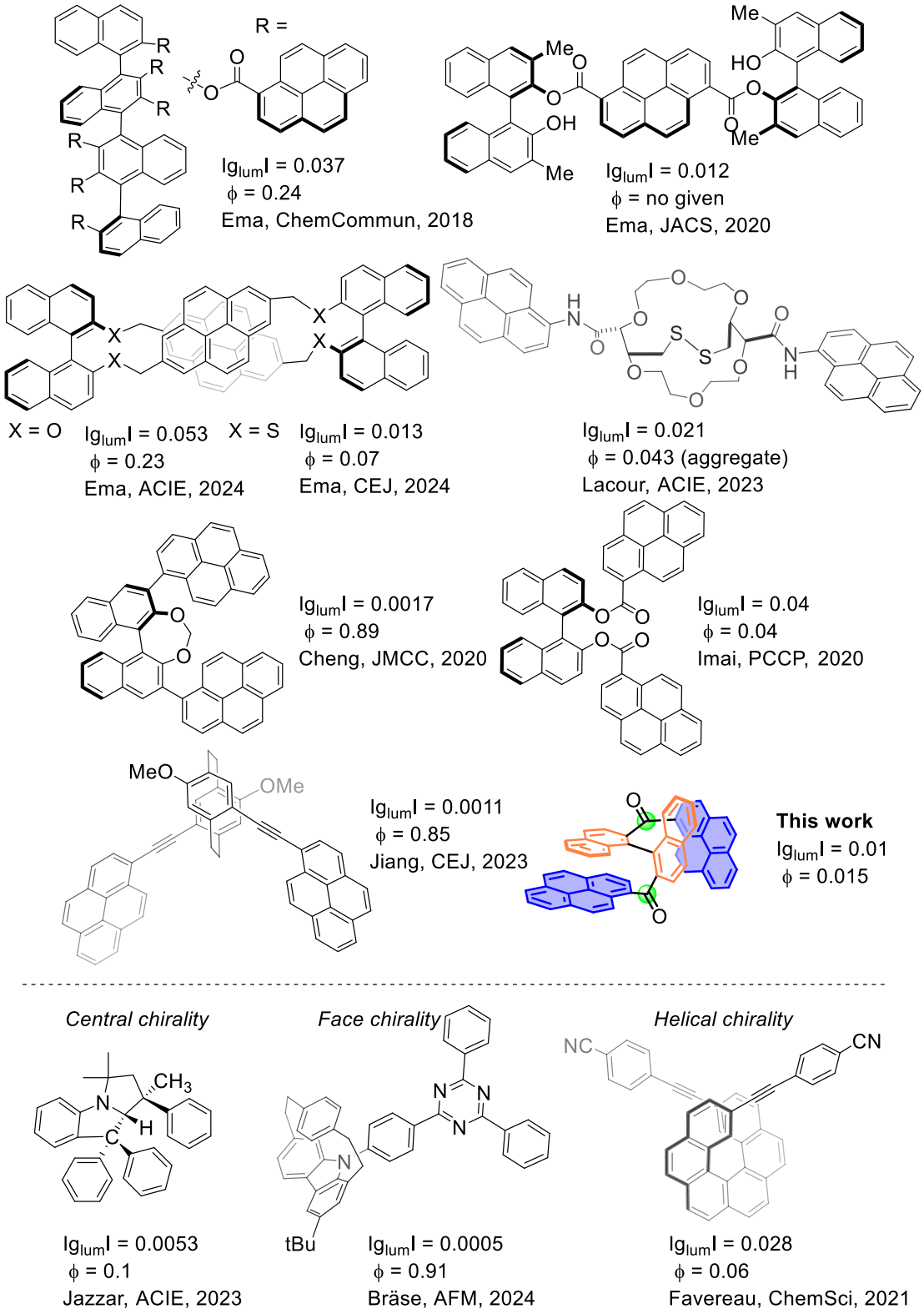

Figure S1. Comparison of the CPL performance among the selected chiral organic molecules containing pyrene and other chiral molecules.[5-17]

Synthesis of (*R*)-/(*S*)-**BiPyCO** and **PyCO**.

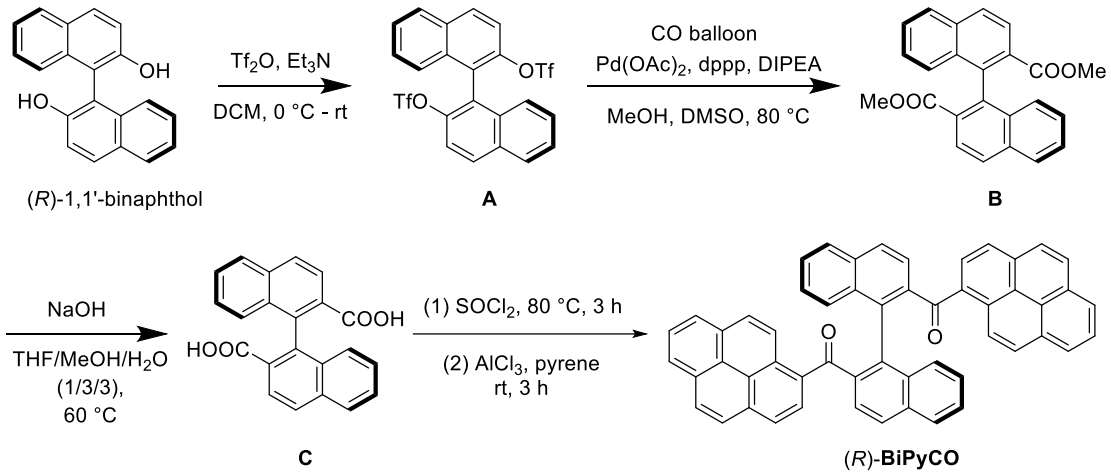

Scheme S1. The synthetic route of (*R*)-**BiPyCO**. The (*S*)-**BiPyCO** was prepared according to the same route but (*S*)-1,1'-binaphthol was used as the starting material.

Preparation of intermediate **A**:[18] In a 500 mL round-bottom flask, (*R*)-1,1'-binaphthol (42.9 g, 150.0 mmol) was added, followed by the addition of dichloromethane (300 mL) and triethylamine (62.5 mL, 450 mmol) to dissolve the solid under stirring conditions. The flask was then placed in an ice-water bath, trifluoromethanesulfonic anhydride (55.5 mL, 330.0 mmol) was gradually dropped into the above solution using a constant-pressure dropping funnel. After the addition was complete, the reaction was allowed to proceed overnight. Upon completion of the reaction, the mixture was condensed and purified by column chromatography using petroleum ether as an eluent, yielding white solid **A** (80.43 g, 146.2 mmol) with

a yield of 97.5%.

Preparation of intermediate **B**:[19] Under a carbon monoxide atmosphere (using a CO balloon), dppp [1,3-bis(diphenylphosphino)propane] (2.475 g, 6 mmol) and $Pd(OAc)_2$ (1.347 g, 6 mmol) were added to a 1000 mL three-neck flask with a reflux condenser. In a separate beaker (1000 mL), compound **A** (22.0 g, 60 mmol) was dissolved in a mixed solution of DMSO (330 mL), MeOH (121.5 mL), and DIPEA (45 mL, 4.4 equiv, 264 mmol). The resulting solution was injected into the above three-neck flask under stirring conditions. After completion, the mixture was placed into the preheated oil bath of 80 °C for three days. Upon completion of the reaction, the mixture was allowed to cool to room temperature. The cooled reaction mixture was then poured into a saturated sodium chloride solution and stirred for one hour to facilitate the precipitation of the solid. The solid was collected by filtration, and the residue was dissolved in dichloromethane and dried over Na_2SO_4. After removing the desiccant and the filter was condensed, the resulting residue was purified by column chromatography on silica gel with the eluent (petroleum ether and ethyl acetate, 20/1, v/v). This process yielded white solid **B** (18.20 g, 49.18 mmol) with a yield of 82%, R_f = 0.33. **^{1}H NMR** ($CDCl_3$, 500 MHz) δ 8.18 (d, *J* = 8.7 Hz, 2H), 8.00 (d, *J* = 8.7 Hz, 2H), 7.94 (d, *J* = 8.3 Hz, 2H), 7.51

(dd, *J* = 8.0,7.1 Hz, 2H), 7.27-7.19 (m, 2H), 7.07 (d, *J* = 8.6 Hz, 2H), 3.48 (s, 6H) ppm; **^{13}C NMR** ($CDCl_3$, 125.8 MHz) δ 167.2, 140.3, 134.9, 132.9, 128.0, 127.9, 127.7, 127.3, 127.2, 126.7, 125.9, 51.9 ppm. **HPLC** analysis: > 99% ee (column: IG-3, Daicel Chemical Industries, Ltd.; eluent: hexanes/isopropanol = 95/5; flow rate: 1.0 mL/min; detection: UV 254 nm).

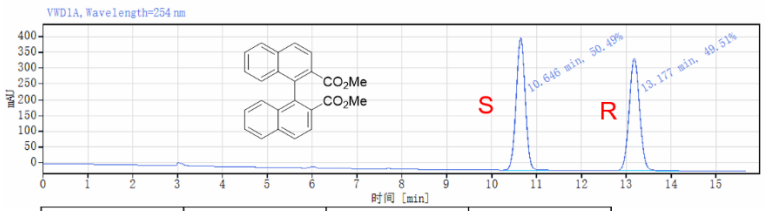

peak	RT [min]	Area %	Area
1	10.646	50.49	5897.3
2	13.177	49.51	5782.5

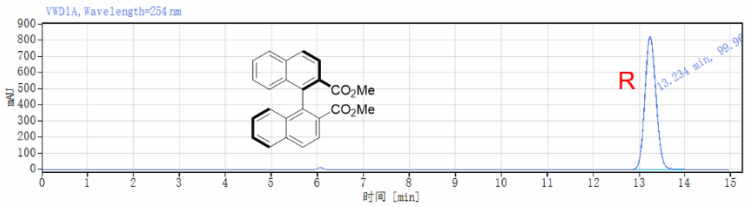

peak	RT [min]	Area %	Area
1	13.234	99.96	14011.0

Figure S2. HPLC results of the key intermediate **B**.

Preparation of intermediate **C**:[20] In a 50 mL round-bottom flask with a reflux condenser, solid **B** (296.5 mg, 0.8 mmol) was added, followed by a mixture of tetrahydrofuran (2 mL), methanol (6 mL) and water (6 mL). under magnetic stirring conditions, sodium hydroxide (256.4 mg, 6.4 mmol) was then introduced to the flask. The mixture was heated at 60 °C for overnight. After the reaction was complete, the solvent was removed under reduced pressure.

The residue was diluted with water (12 mL) and then acidified with 1 mol/L hydrochloric acid, resulting in the formation of a white precipitate. The solid was collected by vacuum filtration and washed extensively with water until neutral. Finally, the solid was placed in a vacuum drying oven at 80 °C to remove any remaining moisture, yielding white solid **C** (270.0 mg, 0.78 mmol) with a yield of 98.6%. **^{1}H NMR** ($CDCl_3$, 500 MHz) δ 8.10 (d, *J* = 8.8 Hz, 2H), 7.94 (d, *J* = 8.8 Hz, 2H), 7.89 (d, *J* = 8.3 Hz, 2H), 7.46 (dd, *J* = 7.7, 7.2 Hz, 2H), 7.12 (dd, *J* = 8.1, 7.2 Hz, 2H), 6.88 (d, *J* = 8.6 Hz, 2H) ppm; **^{13}C NMR** ($CDCl_3$, 125.8 MHz) δ 172.0, 141.7, 135.3, 132.8, 127.9, 127.85, 127.83, 127.4, 126.6, 126.5, 125.6 ppm.

Preparation of (*R*)-**BiNpPy**: In a 50 mL round-bottom flask with a reflux condenser, solid **C** (119.7 mg, 0.35 mmol) was added, followed by the addition of thionyl chloride (2.4 mL) under magnetic stirring conditions. The flask was then placed in an 80 °C oil bath and allowed to reflux for 3 hours. After the reaction was complete, thionyl chloride was removed under reduced pressure conditions. The resulting solid was dissolved in dichloromethane (5 mL), and the distillation was repeated to ensure the complete removal of thionyl chloride. The intermediate (*R*)-[1,1'-binaphthalene]-2,2'-dicarbonyl dichloride was obtained and used directly for the next step.

Under magnetic stirring conditions, the above intermediate (132.7 mg, 0.35 mmol) was dissolved in dichloromethane (6.72 mL), and pyrene (169.9 mg, 0.84 mmol) was then added at room temperature. Anhydrous aluminum chloride powder (233.4 mg, 1.75 mmol) was added in portions. The reaction was then allowed to proceed for 3 hours. Upon completion of the reaction, 3 mol/L dilute hydrochloric acid was added dropwise to quench the reaction. The mixture was extracted with dichloromethane and then dried over Na_2SO_4. After the removing of desiccant and volatiles, the residue was purified by column chromatography on silica gel with the eluent (petroleum ether and ethyl acetate, 10/1, v/v)., yielding a yellow solid (176.6 mg, 0.25 mmol) with a yield of 71%, R_f = 0.22, m.p. 256-258 ˚C. **^{1}H NMR** ($CDCl_3$, 500 MHz) δ 8.34 (d, *J* = 9.3 Hz, 2H), 8.13 (dd, *J* = 8.4, 8.3 Hz, 4H), 7.98 (dd, *J* = 7.6, 7.6 Hz, 2H), 7.93 (dd, *J* = 8.9, 4.1 Hz, 4H), 7.67-7.59 (m, 6H), 7.44 (d, *J* = 8.5 Hz, 2H), 7.38-7.32 (m, 4H), 7.06-6.96 (m, 4H), 6.73 (dd, *J* = 8.1, 7.2 Hz, 2H) ppm; **^{13}C NMR** ($CDCl_3$, 125.8 MHz) δ 200.2, 139.7, 136.6, 133.6, 133.2, 132.4, 132.1, 130.9, 130.5, 128.7, 128.6, 128.3, 128.0, 127.6, 127.5, 127.4, 126.8, 126.7, 126.3, 126.0, 125.9, 125.59, 125.57, 125.1, 124.1, 123.8, 123.2 ppm. **IR** (KBr, cm^{-1}): 3053, 1952, 1651, 1594; **HRMS** (ESI) m/z: found, 733.21423 [M+Na^+]; calcd for $C_{54}H_{30}O_2$+Na^+, 733.21380.

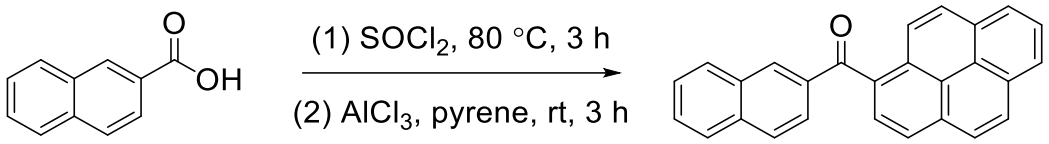

PyCO

Scheme S2. The synthetic route of **PyCO**.

In a 50 mL round-bottom flask with a reflux condenser, 2-naphthoic acid (1.0 g, 5.8 mmol) was added, followed by the addition of thionyl chloride (38.0 mL) under magnetic stirring conditions. The flask was then placed in an 80 °C oil bath and allowed to reflux for 3 hours. After the reaction was complete, thionyl chloride was removed under reduced pressure conditions. The resulting solid was dissolved in dichloromethane (5 mL), and the distillation was repeated to ensure the complete removal of thionyl chloride. The intermediate 2-naphthoyl chloride was obtained and used directly for the next step.

Under magnetic stirring conditions, the above intermediate (5.8 mmol) was dissolved in dichloromethane (50 mL), and pyrene (2.8 g, 13.9 mmol) was then added at room temperature. Anhydrous aluminum chloride powder (1.8 g, 13.9 mmol) was added in portions. The reaction was then allowed to proceed for 3 hours. Upon completion of the reaction, 3 mol/L dilute hydrochloric acid was added dropwise to quench the reaction. The mixture was extracted with dichloromethane and then dried over Na_2SO_4. After the

removing of desiccant and volatiles, the residue was purified by column chromatography on silica gel with the eluent (petroleum ether and ethyl acetate, 10/1, v/v)., yielding a yellow solid (1.69 g, 4.75 mmol) with a yield of 82%, R_f = 0.65, m.p. 108-110 ˚C. **^{1}H NMR** ($CDCl_3$, 500 MHz) δ 8.36 (d, *J* = 9.3 Hz, 1H), 8.30-8.18 (m, 5H), 8.18-8.03 (m, 5H), 7.97 (d, *J* = 8.6 Hz, 1H), 7.92 (d, *J* = 8.2 Hz, 1H), 7.79 (d, *J* = 8.3 Hz, 1H), 7.61 (dd, *J* = 7.8, 7.3 Hz, 1H), 7.50 (dd, *J* = 7.9, 7.2 Hz, 1H) ppm; **^{13}C NMR** ($CDCl_3$, 125.8 MHz) δ 198.5, 136.1, 135.7, 133.5, 133.2, 133.1, 132.4, 131.2, 130.7, 129.8, 129.7, 129.1, 128.9, 128.7, 128.5, 127.8, 127.3,127.0, 126.8, 126.4, 126.1, 126.0, 125.6, 124.9, 124.8, 124.5, 123.9 ppm. **IR** (KBr, cm^{-1}): 3052, 1923, 1648, 1501; **HRMS** (ESI) m/z: found, 379.10962 [M+Na^+]; calcd for $C_{27}H_{16}O$+ Na^+, 379.10934.

Cultivation of single crystals

Single crystals of (*R*)-**BiPyCO** and **PyCO** were obtained through the slow evaporation utilizing a mixed solution of dichloromethane and *n*-hexane. (*R*)-**BiPyCO** exhibited a block form, while **PyCO** presented as a long sheet-like solid. These crystallized forms are suitable for X-ray crystal diffraction.

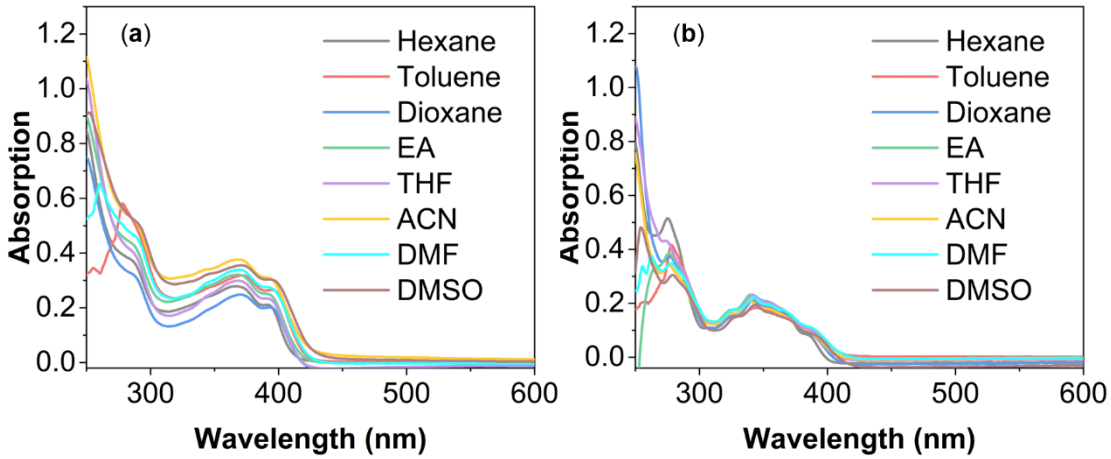

Figure S3. UV-vis spectra of (*R*)-**BiPyCO** (a) and **PyCO** (b) in different solvents at 10^{-5} M.

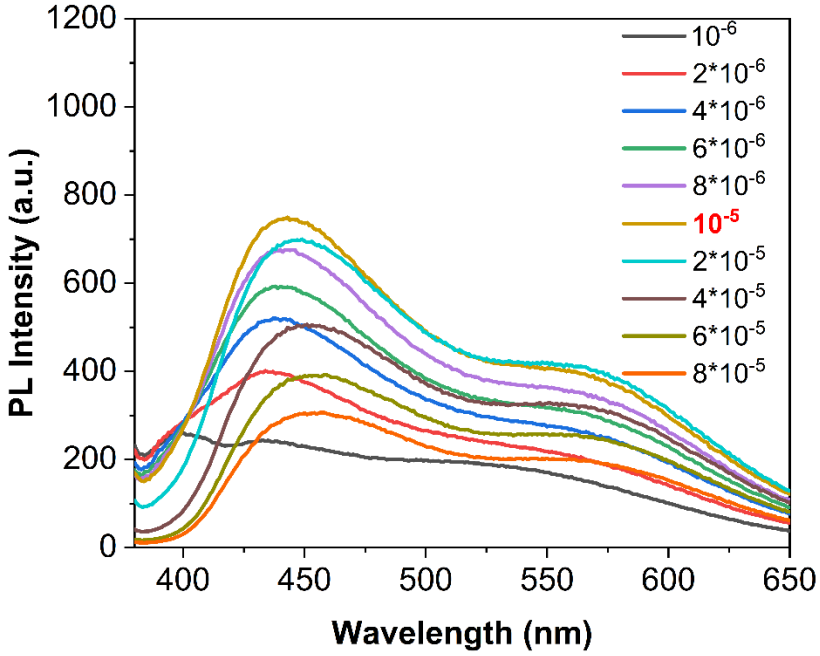

Figure S4. Concentration optimization of (*R*)-**BiPyCO** in acetonitrile by analyzing the intensities of fluorescence spectra.

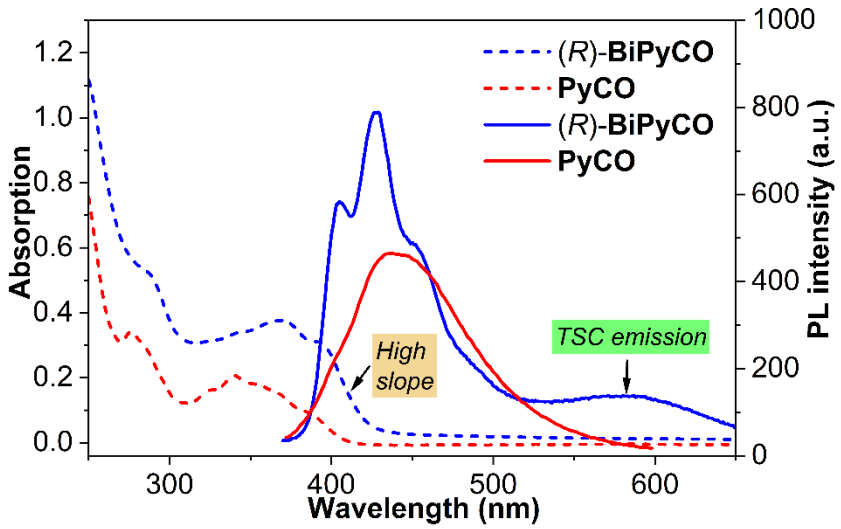

Figure S5. Comparison of UV absorption and fluorescence emission spectra in acetonitrile.

Table S1. Comparison of UV-vis and fluorescence spectra tested in various solvents at the concentration of 10^{-5} M.

(*R*)-**BiPyCO**	Spectra data			
	UV-vis	PL		
solvent	λ_{abs} (nm)	$\lambda_{em1}/\lambda_{em2}$ (nm)	I_1/I_2 (a.u.)	Φ_{PL} (%)
Hex	393, 367	441/550	164/57	2
Toluene	397, 372	450/562	105/40	1.5
Diox	395, 371	438/572	170/56	3.4
EA	393, 369	431/560	93/60	1.1
THF	393, 370	439/568	151/56	1.1
ACN	393, 369	429/571	789/138	8.7
DMF	396, 369	436/578	107/92	4.2
DMSO	397, 370	439/562	220/113	4.1
PyCO	*continued*			
Hex	385, 341, 324	419/-	762/-	2.8
Toluene	391, 345, 327	435/-	335/-	3.2
Diox	390, 342, 326	431/-	533/-	9.6
EA	387, 341, 324	435/-	477/-	2.8
THF	388, 342, 325	433/-	478/-	2.0
ACN	387, 339, 324	438/-	464/-	12.3
DMF	389, 342, 325	443/-	532/-	11.7
DMSO	388, 342, 328	454/-	443/-	6.6

NOTE: Used abbreviations of solvents: hexane (Hex), 1,4-dioxane (Diox), ethyl acetate (EA), tetrahydrofuran (THF), acetonitrile (ACN), *N*,*N*-dimethylformamide (DMF) and dimethyl sulfoxide (DMSO). PL Intensity (*I*), water fraction (f_w).

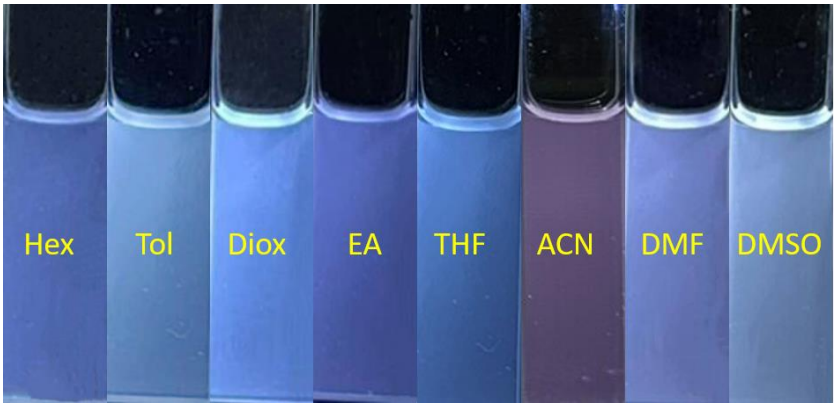

Figure S6. The fluorescent pictures of (*R*)-**BiPyCO** in different solvents at 10^{-5} M under 365 nm UV light.

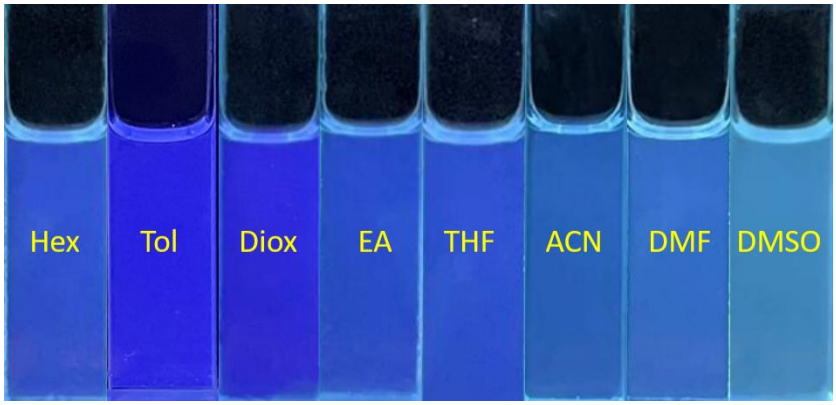

Figure S7. The fluorescent pictures of **PyCO** in different solvents at 10^{-5} M under 365 nm UV light.

Table S2 Summary of fluorescence spectral data of (*R*)-**BiPyCO** and **PyCO** in ACN/H_2O mixtures (10^{-5} M) at different water fractions (f_w).

Entry	(*R*)-**BiPyCO**	**PyCO**

f_w (%)	$\lambda_{em1}/\lambda_{em2}$ (nm)	I_1/I_2 (a.u.)	Φ_{PL}	λ_{em}(max, nm)	I (a.u.)	Φ_{PL}
0	427/573	828/147	8.7%	436	465	12.3%
10	428/586	728/160	3.4%	439	496	2.5%
20	430/580	691/134	3.8%	441	480	2.0%
30	429/582	583/132	2.3%	444	476	3.2%
40	430/590	510/127	1.5%	443	445	3.0%
50	431/587	408/118	3.6%	446	412	2.5%
60	431/512	342/605	1.4%	441	285	1.6%
70	-/514	-/817	0.8%	436	213	0.9%
80	-/520	-/818	1.3%	510	521	1.0%
90	-/519	-/798	1.0%	507	886	0.8%
99	-/515	-/750	0.5%	501	854	0.6%

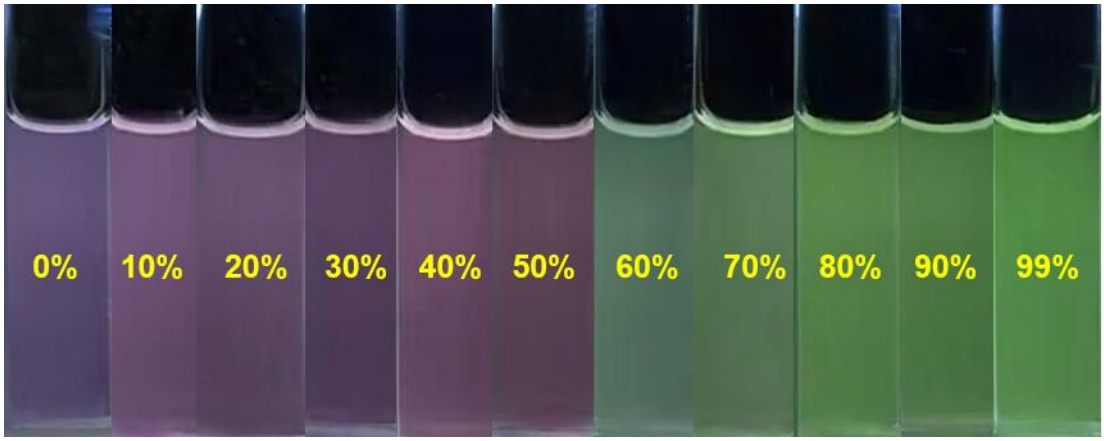

Figure S8. The fluorescent pictures of (*R*)-**BiPyCO** in ACN/H_2O mixtures at different f_w at 10^{-5} M under 365 nm UV light.

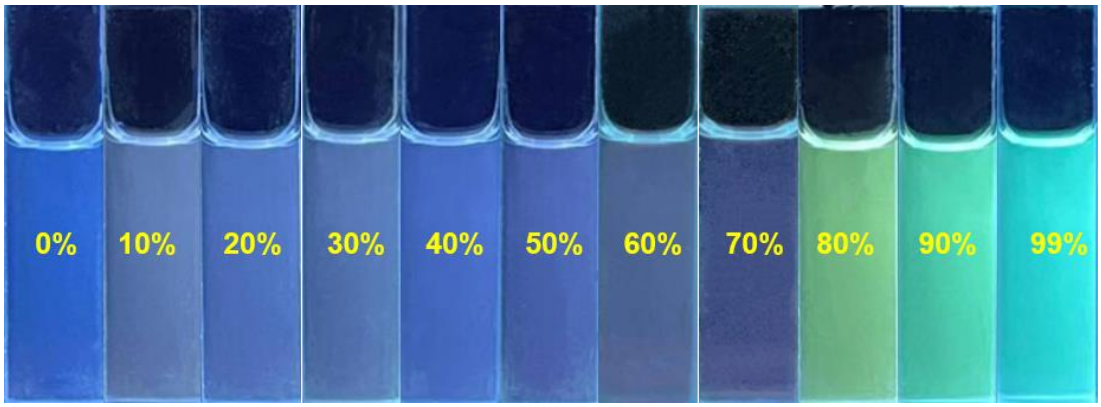

Figure S9. The fluorescent pictures of **PyCO** in ACN/H_2O mixtures at different f_w at 10^{-5} M under 365 nm UV light.

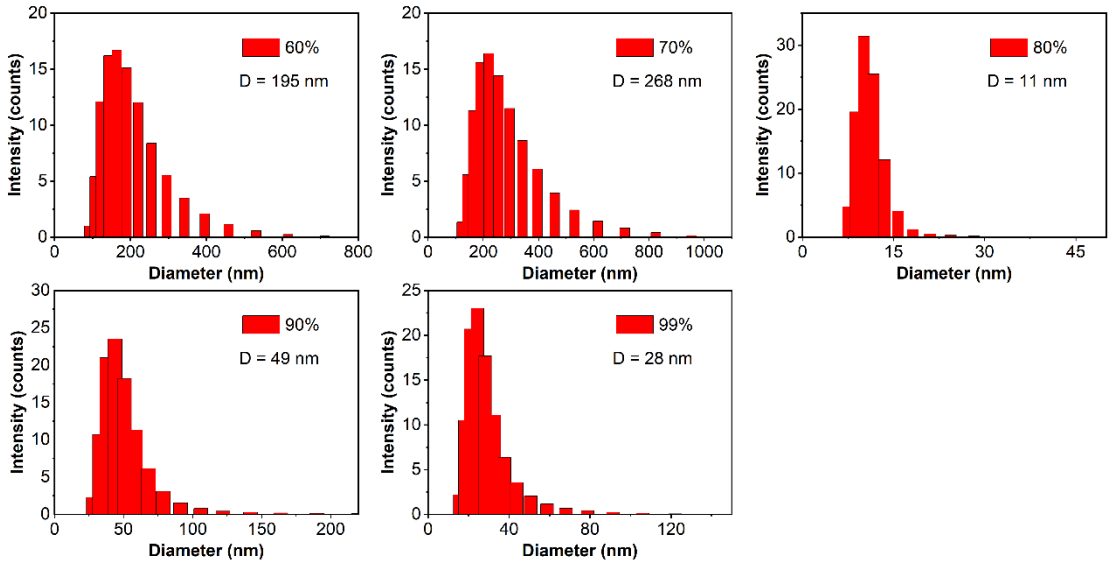

Figure S10. Particle size distribution of (*R*)-**BiPyCO** aggregates formed in ACN/H_2O mixtures (10^{-5} M) at different f_w measured by DLS method.

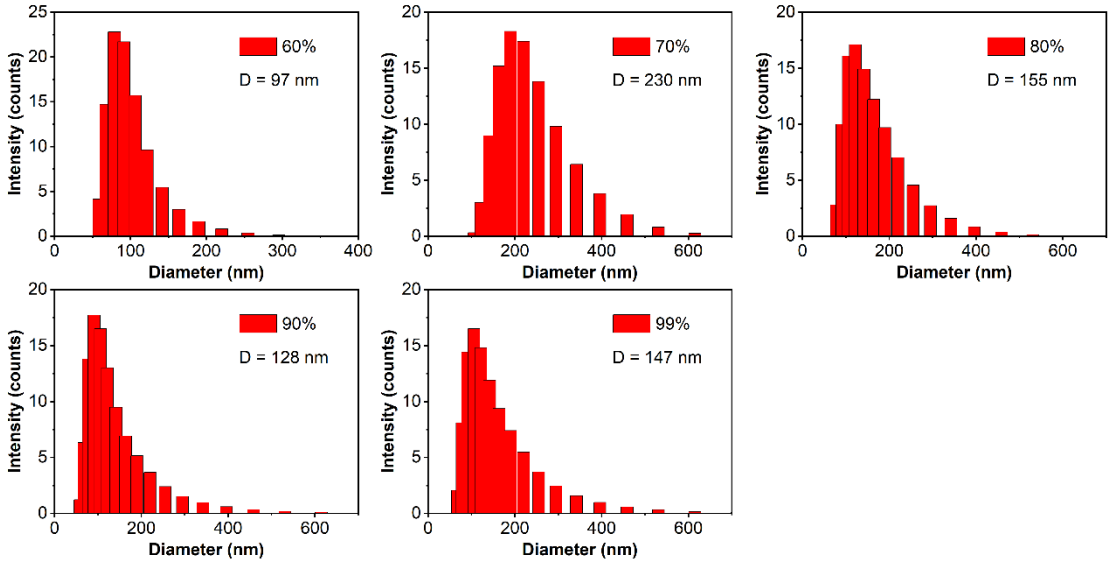

Figure S11. Particle size distribution of **PyCO** aggregates formed in ACN/H_2O mixtures (10^{-5} M) at different f_w measured by DLS method.

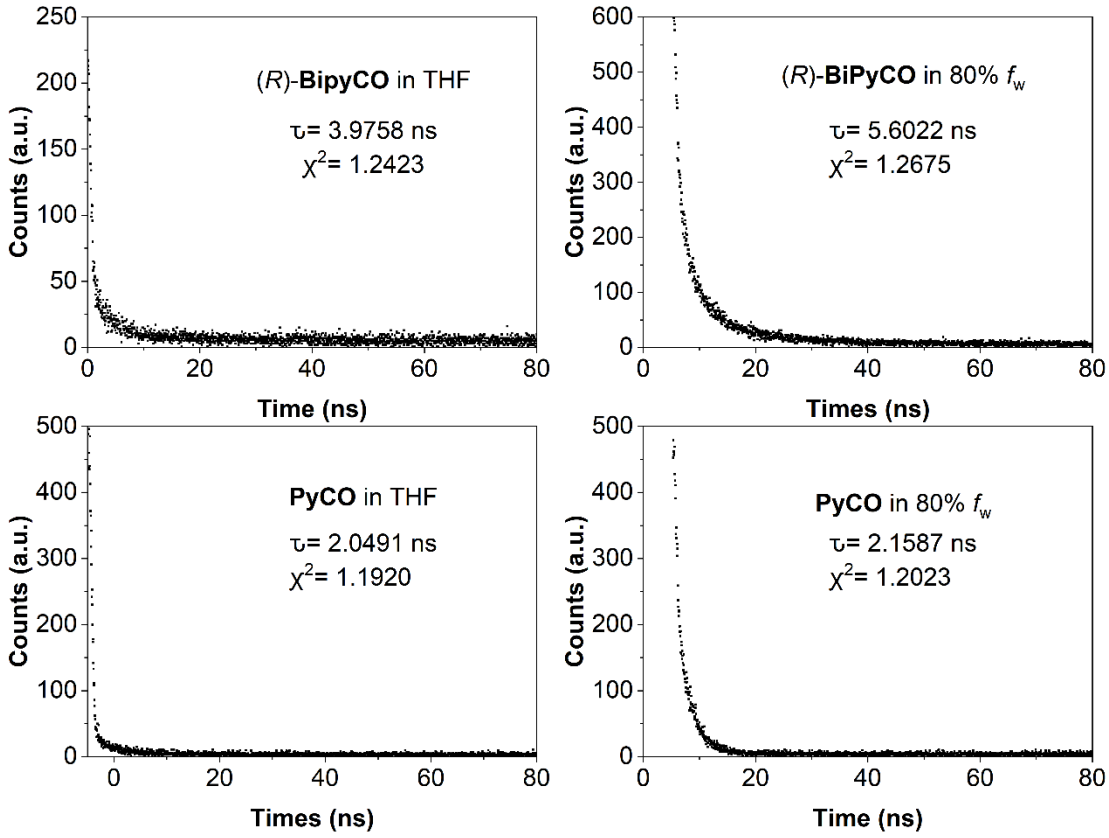

Figure S12. Time-resolved FL decay curves for different compounds in solution and aggregated states.

Table S3 Comparison of maximum emission peaks under different states.

States	(*R*)-**BiPyCO** (λ_{max}, nm)	**PyCO** (λ_{max}, nm)	Δ (nm)
Powder	472	476	4
Crystal	475, 499 (acromion)	493	18, 6
Aggregate (10^{-5} M)	520 (80% f_w)	507 (90% f_w)	13

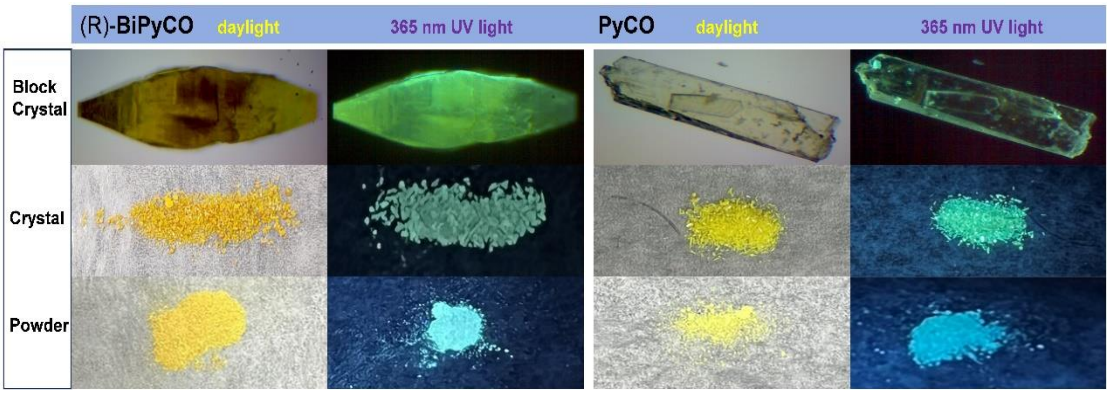

Figure S13. The pictures of (*R*)-**BiPyCO** and **PyCO** at crystal and powder states under daylight and 365 nm UV light.

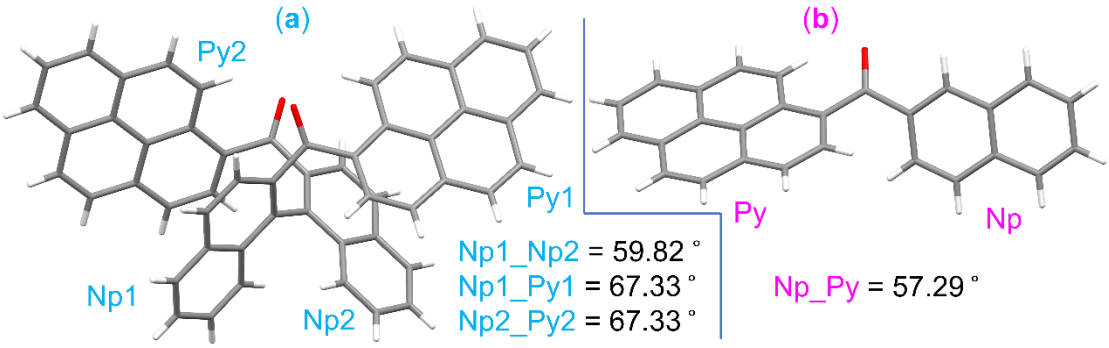

Figure S14. X-ray crystal structures of (*R*)-**BiPyCO** and **PyCO**, and the relevant dihedral angles. The shown type is capped sticks (H, white; C, grey; O, red).

Table S4 Crystal data and structure refinement for (*R*)-**BiPyCO** and **PyCO**.

Identification code	(*R*)-**BiPyCO**	**PyCO**
Empirical formula	$C_{54}H_{30}O_2$	$C_{27}H_{16}O$
Formula weight	710.78	356.40
Temperature/K	273.15	273.15
Crystal system	tetragonal	triclinic
Space group	$P4_12_12$	P-1
a/Å	8.1952(9)	6.2290(7)
b/Å	8.1952(9)	8.9609(11)
c/Å	52.758(8)	17.0384(19)
α/°	90	103.426(3)

β/°	90	94.535(3)
γ/°	90	100.782(3)
Volume/Å^3	3543.3(9)	901.22(18)
Z	4	2
ρ_{calc}g/cm^3	1.332	1.313
μ/mm^{-1}	0.080	0.078
F(000)	1480.0	372.0
Crystal size/mm^3	0.5 × 0.2 × 0.2	0.4 × 0.3 × 0.1
Radiation	MoKα (λ = 0.71073)	MoKα (λ = 0.71073)
2θ range for data collection/°	5.03 to 45.97	4.782 to 50.052
Index ranges	-9 ≤ h ≤ 5, -9 ≤ k ≤ 8, -57 ≤ l ≤ 53	-7 ≤ h ≤ 7, -10 ≤ k ≤ 10, -20 ≤ l ≤ 20
Reflections collected	8988	9502
Independent reflections	2441 [R_{int} = 0.0418, R_{sigma} = 0.0484]	3171 [R_{int} = 0.0326, R_{sigma} = 0.0417]
Data/restraints/parameters	2441/0/254	3171/0/254
Goodness-of-fit on F_2	1.063	1.019
Final R indexes [I>=2σ (I)]	R_1 = 0.0537, wR_2 = 0.1328	R_1 = 0.0465, wR_2 = 0.1107
Final R indexes [all data]	R_1 = 0.0793, wR_2 = 0.1470	R_1 = 0.0968, wR_2 = 0.1367
Largest diff. peak/hole / e Å^{-3}	0.15/-0.14	0.16/-0.12

Note: The absolute configuration was not able to be determined by the X-ray single crystal analysis for (*R*)-**BiPyCO**.

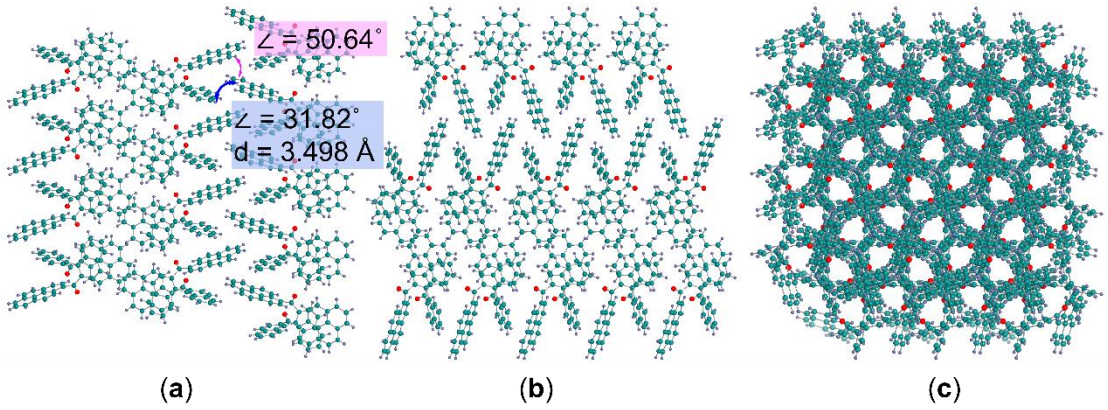

Figure S15. Crystal stacking diagram of (*R*)-**BiPyCO** viewed along

different directions (axis a, b and c). O, red; H, blue-grey; C, teal.

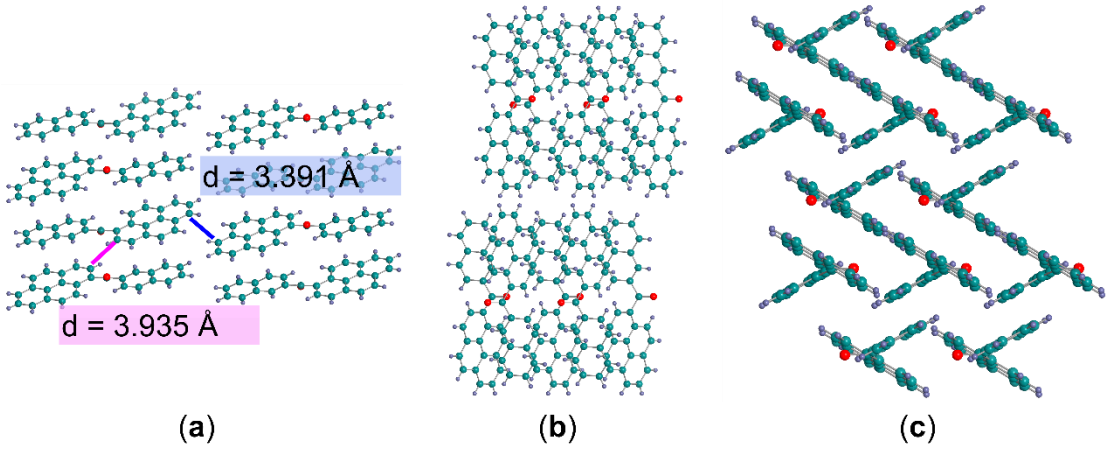

Figure S16. Crystal stacking diagram of **PyCO** viewed along different directions (axis a, b and c). O, red; H, blue-grey; C, teal.

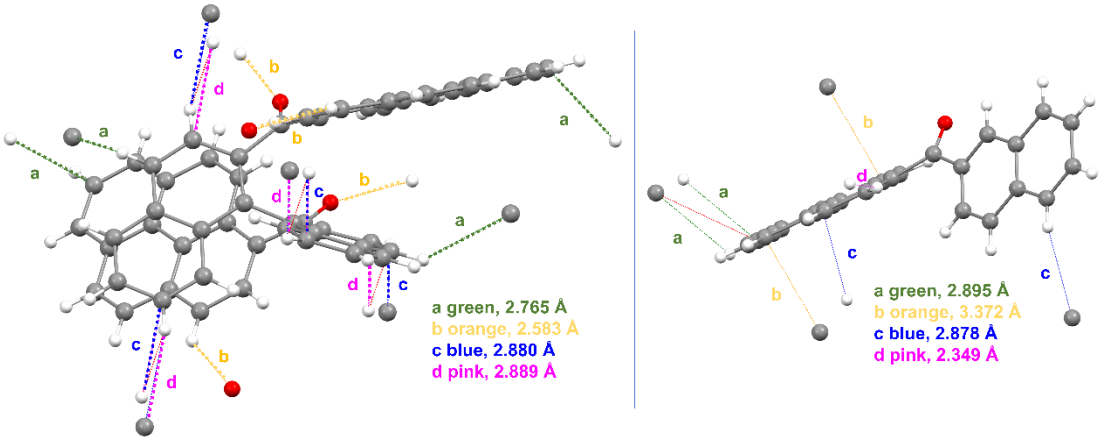

Figure S17. Intermolecular interactions for X-ray structures of (*R*)-**BiPyCO** (left image) and **PyCO** (right image) calculated by the *Mercury 4.3.1* software. In order to clarifying the complex intermolecular weak interactions, only the central molecular structure is displayed as the research object, and while the surrounding molecules only show the partial atoms which have weak interactions to the central molecule.

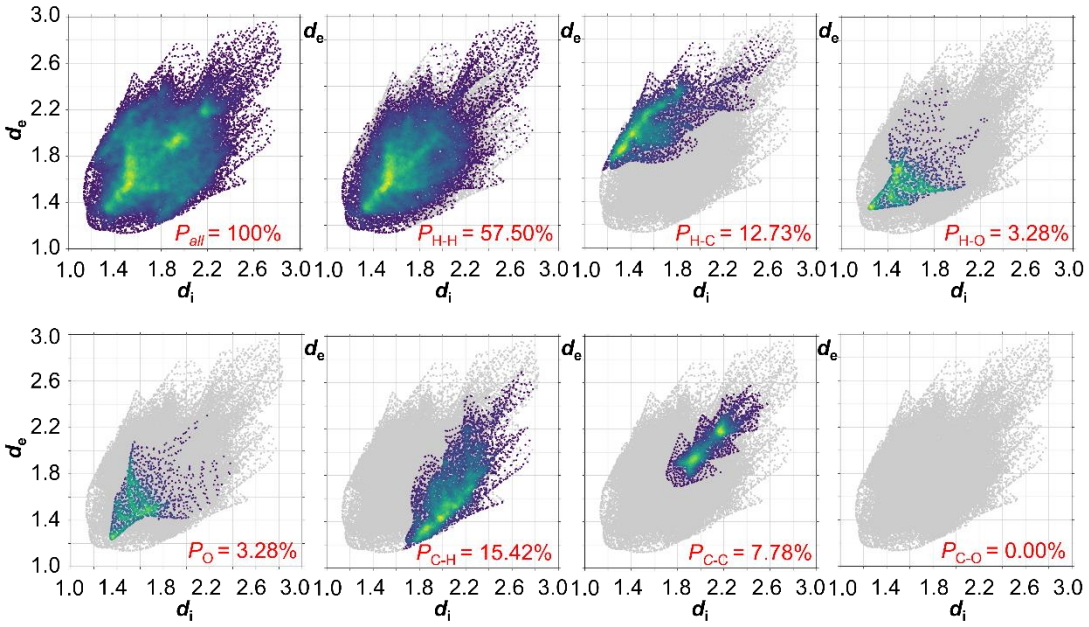

Figure S18. The decomposed fingerprint plots of (*R*)-**BiPyCO**. The full fingerprints were appeared in the first picture and marked the sum of proportion (P_{all}), and as grey shadow underneath decomposed plots. P_O = proportion of oxygen-involved intermolecular interaction to total intermolecular interaction; The proportions of intermolecular X…Y interaction to total intermolecular interaction were also indicated as $P_{X\text{-}Y}$ (X, Y = H, C and O, X: atoms of the central molecule; Y: atoms of surrounding molecules).

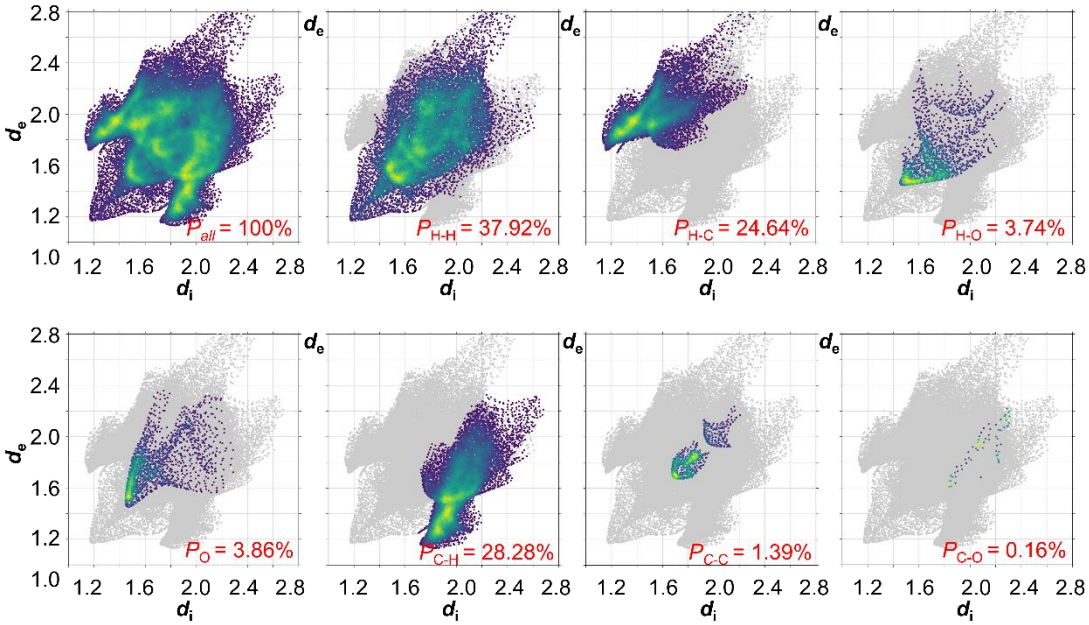

Figure S19. The decomposed fingerprint plots of **PyCO**. The full fingerprints were appeared in the first picture and marked the sum of proportion (P_{all}), and as grey shadow underneath decomposed plots. P_O = proportion of oxygen-involved intermolecular interaction

to total intermolecular interaction; The proportions of intermolecular X…Y interaction to total intermolecular interaction were also indicated as $P_{X\text{-}Y}$ (X, Y = H, C and O, X: atoms of the central molecule; Y: atoms of surrounding molecules).

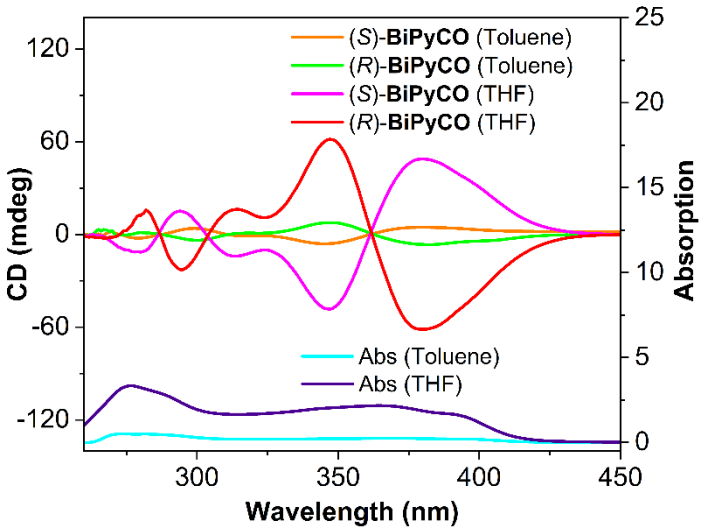

Figure S20. The CD spectra of (*R*)-/(*S*)-**BiPyCO** measured in THF and toluene at 10^{-5} M.

Table S5 Photophysical parameters and B_{CPL} of (*R*)-**BiPyCO** in different system.

Solvent	ε ($M^{-1}cm^{-1}$, λ_{ex}/nm)	Φ (%)	$\lvert g_{lum} \rvert$	B_{CPL} ($M^{-1}cm^{-1}$)
THF	25700 (350)	1.1	0.012	1.7
toluene	28000 (350)	1.5	0.010	2.1
80% f_w	78700 (350)	1.0	0.005	2.0

Table S6 Comparison of different functional theory calculations and experimental results for (*R*)-**BiPyCO**.

Excited state	S1 λ (nm), *f*		S2 λ (nm), *f*	S3 λ (nm), *f*	S4 λ (nm), *f*	S5 λ (nm), *f*
Absorption peaks[a]		394, 370, 334, 317 nm in the scope of 420-250 nm				
B3LYP/6-31G(d,p)[b]	441.96, 0.01560		439.26, 0.10390	407.23, 0.11240	402.82, 0.02150	378.54, 0.11450
CAM-B3LYP/6-31G(d,p)[b]	345.65, 0.47080		343.27, 0.08070	326.70, 0.01220	324.65, 0.02970	314.49, 0.00000
PBE1PBE/6-31G(d,p)[b]	416.73, 0.02380		415.34, 0.15410	384.45, 0.12200	380.88, 0.02890	357.83, 0.12010

[a] The UV-vis absorption peaks of (*R*)-**BiPyCO** in hexanes. [b] The excited calculations were carried out using the optimized

geometries with the corresponding time-dependent (TD)-functionals and GD3 empirical dispersion correction. "λ" is excitation wavelength and "*f*" is oscillator strength.

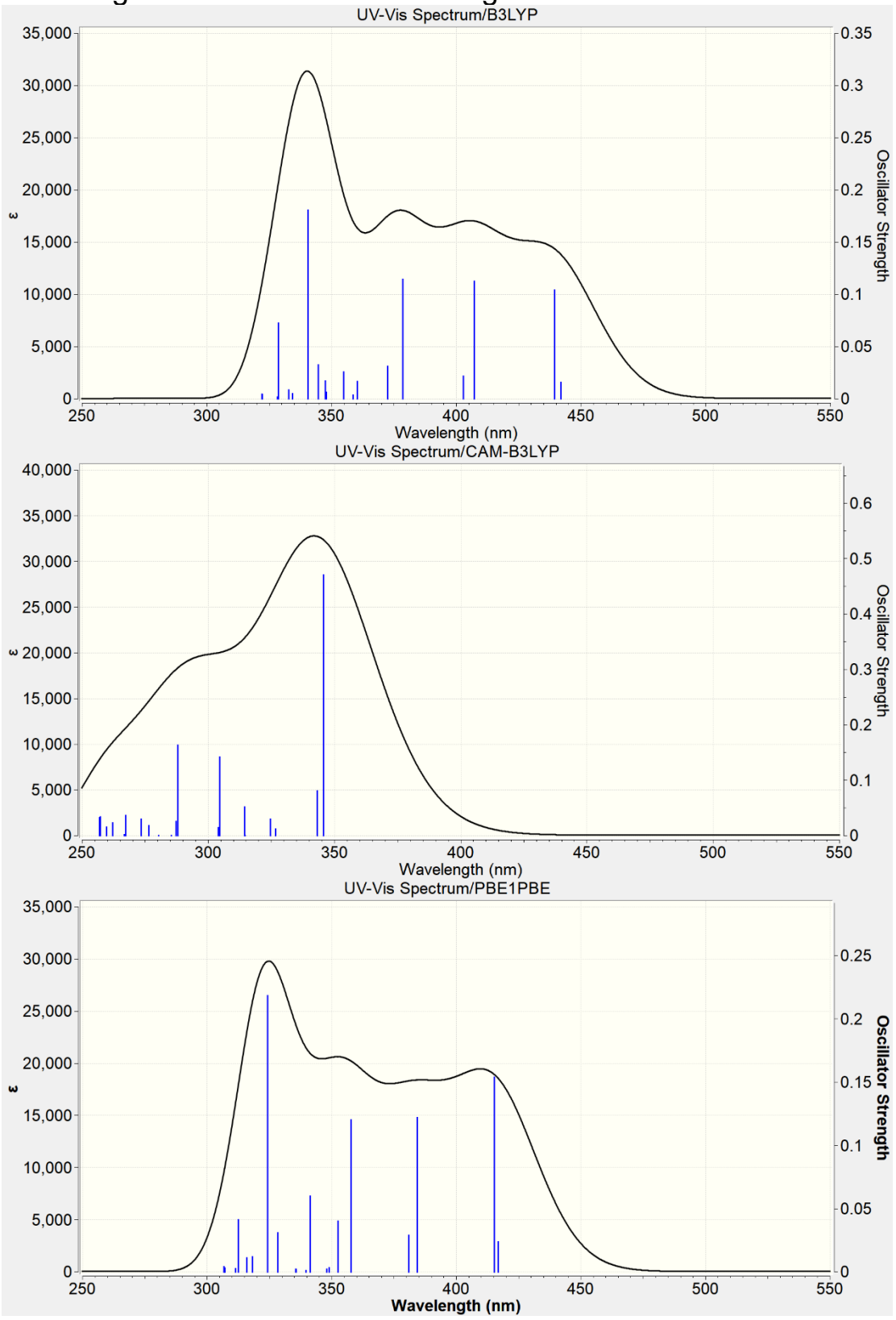

Figure S21. Simulated UV visible absorption spectra using different functionals under gas phase conditions.

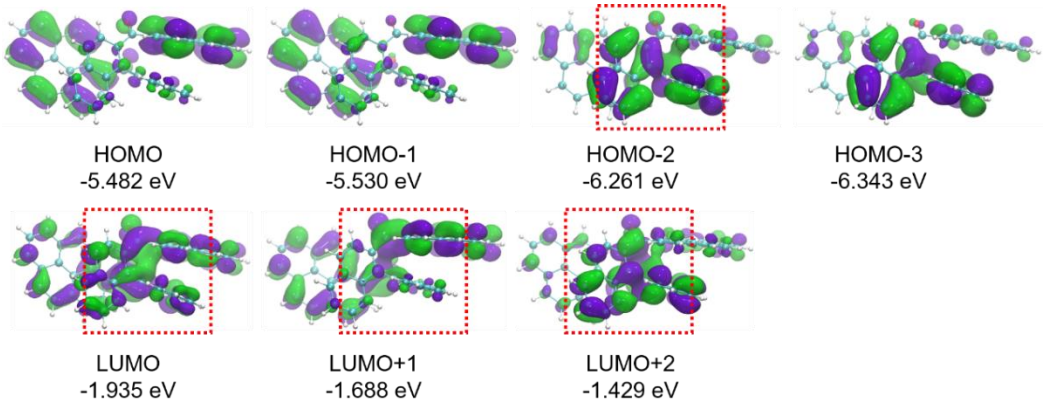

Figure S22. Frontier molecular orbitals of (*R*)-**BiPyCO** in geometry of optimized S0 state at the theory level of PBE0-D3/6-31G(d,p) (isosurface: 0.02. gap = 3.547 eV). Molecular orbitals with through-space conjugation characteristic are highlighted in red dashed boxes.

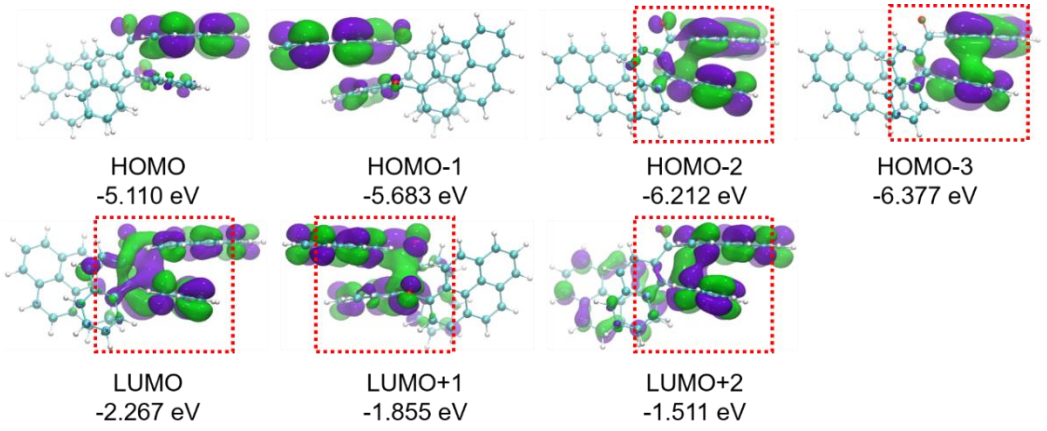

Figure S23. Frontier molecular orbitals of (*R*)-**BiPyCO** in geometry of optimized S1 state at the theory level of TD/PBE0-D3/6-31G(d,p) (isosurface: 0.02. gap = 2.842 eV). Molecular orbitals with through-space conjugation characteristic are highlighted in red dashed boxes.

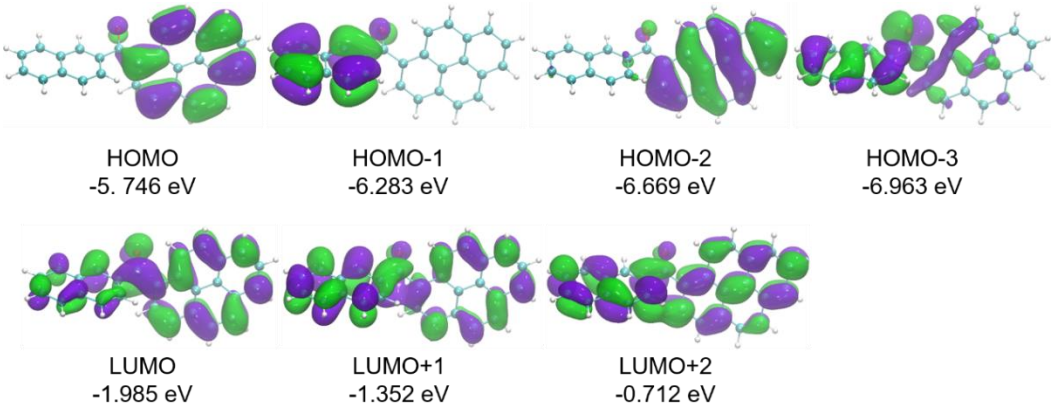

Figure S24. Frontier molecular orbitals of **PyCO** in geometry of optimized S0 state at the theory level of PBE0-D3/6-31G(d,p) (isosurface: 0.02. gap = 3.761 eV).

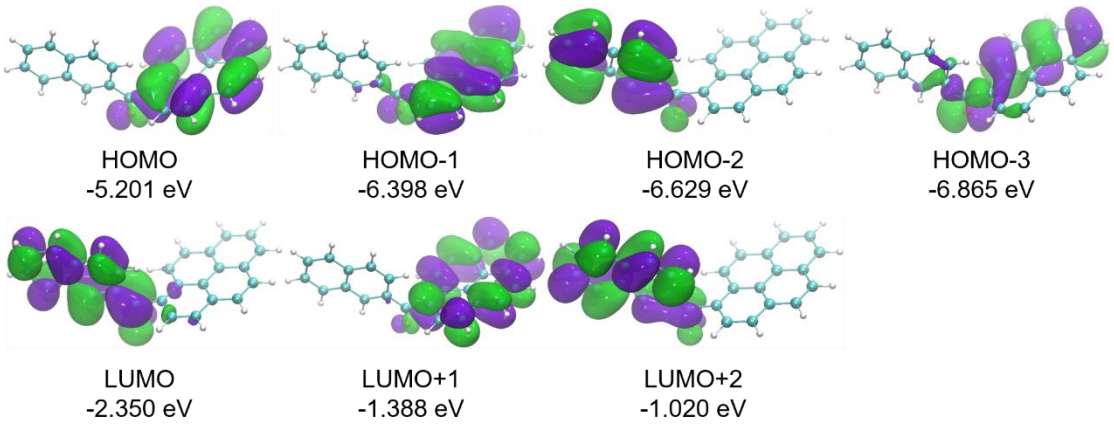

Figure S25. Frontier molecular orbitals of **PyCO** in geometry of optimized S1 state at the theory level of TD/PBE0-D3/6-31G(d,p) (isosurface: 0.02. gap = 2.851 eV). The charge transfer from naphthyl to pyrene ring during de-excitation could exist based on the analysis of LUMO→HOMO.

Table S7 Overview of the relevant transitions for (*R*)-**BiPyCO** and **PyCO** calculated by TD-DFT at PBE0-D3/6-31G(d,p) level.

Product	Transition	λ (nm)	*f*	Orbital Contributions (%)	Type
(*R*)-**BiPyCO**	$S_0 \rightarrow S_1$	416.73	0.02380	H→L, 95.3	LE
	$S_0 \rightarrow S_2$	415.34	0.15410	H-1→L, 95.5	LE
	$S_0 \rightarrow S_3$	384.45	0.12200	H→L+1, 73.8, H→L+2, 20.7	LE
	$S_0 \rightarrow S_4$	380.88	0.02890	H-1→L+1, 72.2, H-1→L+2, 22.7	LE
	$S_0 \rightarrow S_5$	357.83	0.12010	H→L+2, 76.1, H→L+1, 20.2	LE
PyCO	$S_0 \rightarrow S_1$	378.98	0.37650	H→L, 91.5	LE
	$S_0 \rightarrow S_2$	359.79	0.02660	H-3→L, 49.2, H-1→L, 20.9, H-4→L, 12.2	LE
	$S_0 \rightarrow S_3$	334.58	0.05640	H-1→L, 51.4, H-	LE

				3→L, 15.3, H-2→L, 14.0, H→L+2, 5.5	

“H” is HOMO, “L” is LUMO.

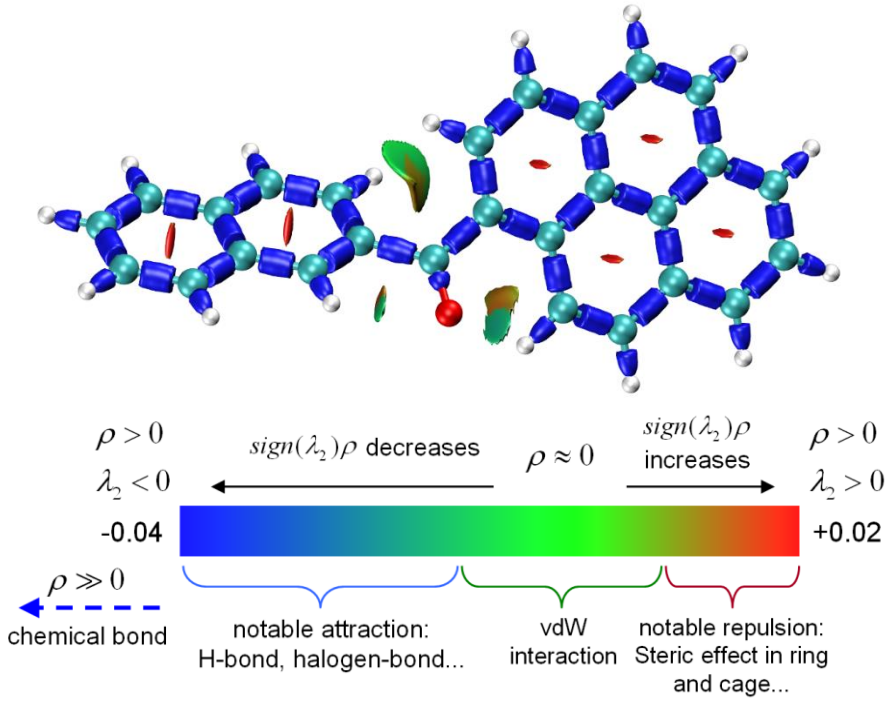

Figure S26. The distribution of IRI isosurfaces for **PyCO** (a.u.).

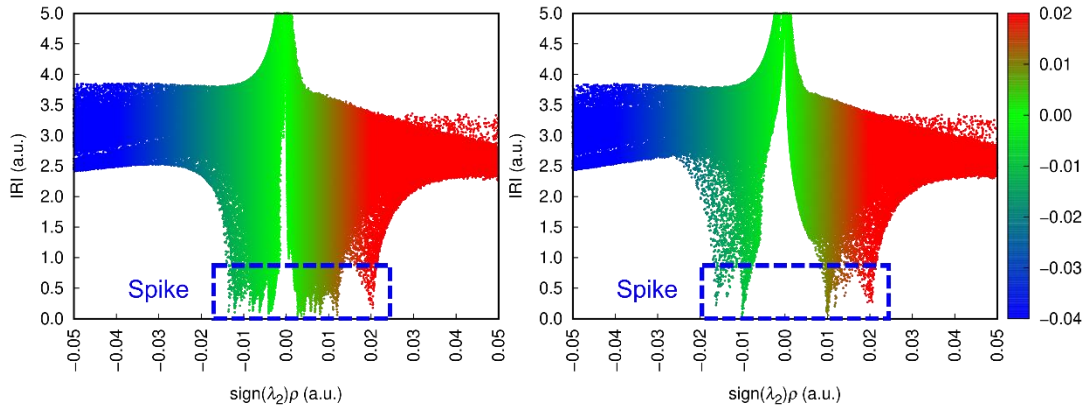

Figure S27. Comparison of scatter plot of IRI versus sign(λ_2)ρ for (*R*)-**BiPyCO** (left) and **PyCO** (right).

Reference

[1] Gaussian 16, *Revision C.01*, M. J. Frisch, G. W. Trucks, H. B. Schlegel, G. E. Scuseria, M. A. Robb, J. R. Cheeseman, G. Scalmani, V. Barone, G. A. Petersson, H. Nakatsuji, X. Li, M. Caricato, A. V. Marenich, J. Bloino, B. G. Janesko, R. Gomperts, B.

Mennucci, H. P. Hratchian, J. V. Ortiz, A. F. Izmaylov, J. L. Sonnenberg, D. Williams-Young, F. Ding, F. Lipparini, F. Egidi, J. Goings, B. Peng, A. Petrone, T. Henderson, D. Ranasinghe, V. G. Zakrzewski, J. Gao, N. Rega, G. Zheng, W. Liang, M. Hada, M. Ehara, K. Toyota, R. Fukuda, J. Hasegawa, M. Ishida, T. Nakajima, Y. Honda, O. Kitao, H. Nakai, T. Vreven, K. Throssell, J. A. Montgomery, Jr., J. E. Peralta, F. Ogliaro, M. J. Bearpark, J. J. Heyd, E. N. Brothers, K. N. Kudin, V. N. Staroverov, T. A. Keith, R. Kobayashi, J. Normand, K. Raghavachari, A. P. Rendell, J. C. Burant, S. S. Iyengar, J. Tomasi, M. Cossi, J. M. Millam, M. Klene, C. Adamo, R. Cammi, J. W. Ochterski, R. L. Martin, K. Morokuma, O. Farkas, J. B. Foresman, and D. J. Fox, Gaussian, Inc., Wallingford CT, **2019**.

[2] (a) M. A. Spackman, D. Jayatilaka, Hirshfeld Surface Analysis, *CrystEngComm,* **2009**, *11*, 19-32.

[3] T. Lu, Q. Chen, Interaction Region Indicator (IRI): A Simple Real Space Function Clearly Revealing Both Chemical Bonds and Weak Interactions, *Chemistry—Methods*, **2021**, *1*, 231-239.

[4] (a) T. Lu, F. Chen, Multiwfn: A Multifunctional Wavefunction Analyzer, *J. Comput. Chem*., **2012**, *33*, 580-592. (http://sobereva.com/multiwfn/). (b) W. Humphrey, A. Dalke, K. Schulten, *J. Molec. Graphics* **1996**, *14*, 33. (http://www.ks.uiuc.edu/Research/vmd/).

[5] K. Takaishi, R. Takehana and T. Ema, Intense excimer CPL of pyrenes linked to a quaternaphthyl, *Chem. Commun.*, 2018, **54**, 1449–1452.

[6] K. Takaishi, K. Iwachido, R. Takehana, M. Uchiyama and T. Ema, Evolving Fluorophores into Circularly Polarized Luminophores with a Chiral Naphthalene Tetramer: Proposal of Excimer Chirality Rule for Circularly Polarized Luminescence, *J. Am. Chem. Soc*., 2019, **141**, 6185–6190.

[7] K. Takaishi, K. Iwachido and T. Ema, Solvent-Induced Sign Inversion of Circularly Polarized Luminescence: Control of Excimer Chirality by Hydrogen Bonding, *J. Am. Chem. Soc.*, 2020, **142**, 1774-1779.

[8] K. Takaishi, S. Murakami, F. Yoshinami and T. Ema, Binaphthyl-Bridged Pyrenophanes: Intense Circularly Polarized Luminescence Based on a D2 Symmetry Strategy, *Angew. Chem. Int. Ed.*, 2022,

61, e202204609.

[9] K. Takaishi, F. Yoshinami, Y. Sato and T. Ema, Temperature-Induced Sign Inversion of Circularly Polarized Luminescence of Binaphthyl-Bridged Tetrathiapyrenophanes, *Chem. Eur. J.*, 2024, **30**, e202400866.

[10] K.-F. Zhang, N. Saleh, M. Swierczewski, A. Rosspeintner, F. Zinna, G. Pescitelli, C. Besnard, L. Guénée, T. Bürgi and J. Lacour, Multistate Aggregation-Induced Chiroptical Properties of Enantiopure Disulfide-Mediated Bispyrene Macrocycles, *Angew. Chem. Int. Ed*., 2023, **62**, e202304075.

[11] X. Zhang, Z. Xu, Y. Zhang, Y. Quan and Y. Cheng, High brightness circularly polarized electroluminescence from conjugated polymer F8BT induced by chiral binaphthyl-pyrene, *J. Mater. Chem. C*, 2020, **8**, 15669-15676.

[12] H. Okada, N. Hara, D. Kaji, M. Shizuma, M. Fujuiki and Y. Imai, Excimer-origin CPL vs. monomer-origin magnetic CPL in photo-excited chiral binaphthyl-ester-pyrenes: critical role of ester direction, *Phys. Chem. Chem. Phys*., 2020, **22**, 13862-13866.

[13] C. Wang, T. Jiang and X. Ma, Circularly polarized luminescence induced by excimer based on pyrene-modified binaphthol. *Chinese Chem. Lett.*, 2020, **31**, 2921–2924.

[14] Z. Lian, L. Liu, J. He, S. Fan, S. Guo, X. Li, G. Liu, Y. Fan, X. Chen, M. Li, C. Chen and H. Jiang, Structurally Diverse Pyrene-decorated Planar Chiral [2,2]Paracyclophanes with Tunable Circularly Polarized Luminescence between Monomer and Excimer, *Chem. Eur. J.*, 2024, **30**, e202303819.

[15] J. Lorkowski, D. Bouetard, P. Yorkgitis, M. Gembicky, T. Roisnel, N. Vanthuyne, D. Munz, L. Favereau, G. Bertrand, M. Mauduit and R. Jazzar, Circularly Polarized Luminescence from Cyclic (Alkyl)(Amino) Carbene Derived Propellers, *Angew. Chem. Int. Ed.*, 2023, **62**, e202305404.

[16] J. Seibert, Y. Xu, H. Hafeez, J. Podlech, L. Favereau, E. Spuling, C. Waldhelm, M. Nieger, O. Fuhr, Z. Hassan, J. Crassous, I. D. W. Samuel, E. Zysman-Colman and S. Bräse, A Novel Carbazolophane: A Comparison of the Performance of Two Planar Chiral CP-TADF Emitters, *Adv. Funct. Mater.*, 2024, **34**, 2401956.

[17] K. Dhbaibi, L. Abella, S. Meunier-Della-Gatta, T. Roisnel, N. Vanthuyne, B. Jamoussi, G. Pieters, B. Racine, E. Quesnel, J. Autschbach, J. Crassous and L. Favereau, Achieving high circularly polarized luminescence with push–pull helicenic systems: from rationalized design to top-emission CP-OLED applications, *Chem. Sci.***,** 2021,**12**, 5522-5533.

[18] T. Ooi, M. Kameda, K. Maruoka, Design of *N*-Spiro C_2-Symmetric Chiral Quaternary Ammonium Bromides as Novel Chiral Phase-Transfer Catalysts: Synthesis and Application to Practical Asymmetric Synthesis of *r*-Amino Acids. *J. Am. Chem. Soc.* **2003**, *125*, 5139-5151.

[19] T. Ohta, M. Ito, K. Inagaki, H. Takaya, A Convenient Synthesis of Optically Pure Dimethyl 1,1'-Binaphthalene-2,2'-dicarboxylate from 1,1'-binaphthalene-2,2'-diol. *Tetrahedron Lett*., **1993**, *34*, 1615-1616.

[20] M. Seki, S.-i. Yamada, T. Kuroda, R. Imashiro, T. Shimizu, A Practical Synthesis of C2-Symmetric Chiral Binaphthyl Ketone Catalyst. *Synthesis* **2000**, *2000*, 1677–1680.

Cartesian Coordinates

DFT optimized S0 structure (ground state)

(*R*)-**BiPyCO** in S0 state

Atom	X	Y	Z
C	6.51371900	-0.72567500	-0.16275500
C	6.76715200	0.41080400	-0.99850800
H	7.76828600	0.83439000	-1.00494200
C	5.20683400	-1.29024700	-0.15171400
C	7.50939300	-1.29219000	0.64162500
C	4.17279400	-0.72263800	-0.94932700
C	4.93400100	-2.41778700	0.67036200
C	5.78529800	0.95147600	-1.76378900
C	7.23327200	-2.39394700	1.44422100
H	8.50656100	-0.85962100	0.63132000
C	2.85932100	-1.27415100	-0.91488000
C	4.45810600	0.41215800	-1.76088000
C	3.61076200	-2.96015200	0.66739000
C	5.96126400	-2.95255500	1.45922500
H	5.98555400	1.81743900	-2.38918200
H	8.01777900	-2.82119200	2.06203100
C	1.83696700	-0.61783200	-1.63690100
C	2.61800400	-2.41850500	-0.08496900
C	3.42942600	0.98618100	-2.51438900
H	3.40123600	-3.81937500	1.29911000
H	5.74942000	-3.81472100	2.08621900
C	0.41623900	-1.06625300	-1.58673200
C	2.13862800	0.49450300	-2.42612000
H	1.62143300	-2.83777200	-0.04659400
H	3.64245200	1.85174500	-3.13492500
O	0.09423200	-2.23663100	-1.71768600
C	-0.64832800	-0.01493500	-1.42710600
H	1.33604100	0.98723800	-2.96744700
C	-0.56317200	1.01032700	-0.49016600
C	-1.80655300	-0.16154900	-2.22861700
C	-1.61810200	1.97070900	-0.40306100
C	0.56327100	1.01041700	0.48983200
H	-1.85585200	-1.01305000	-2.89907200
C	-2.84080600	0.72753700	-2.13220800
C	-2.77180800	1.81701100	-1.22907000
C	-1.58260500	3.05093500	0.51499900
C	1.61808900	1.97093100	0.40275600
C	0.64844800	-0.01474300	1.42687000
H	-3.73620700	0.59991500	-2.73423000
C	-3.83839000	2.73984700	-1.10368800
H	-0.71531900	3.16577600	1.15686200
C	-2.62336000	3.94281800	0.59686900
C	2.77173200	1.81743800	1.22889100
C	1.58251400	3.05112700	-0.51533500
C	-0.41610000	-1.06606700	1.58654000

C	1.80662300	-0.16117300	2.22848800
H	-4.72141700	2.59900200	-1.72111400
C	-3.76717300	3.78263100	-0.21392300
H	-2.57260400	4.76878200	1.30031100
C	2.84078300	0.72802200	2.13210300
C	3.83818600	2.74042900	1.10358700
H	0.71528100	3.16580400	-1.15729900
C	2.62313600	3.94317800	-0.59711400
O	-0.09406600	-2.23644900	1.71744300
C	-1.83681500	-0.61764400	1.63676600
H	1.85594900	-1.01260300	2.89903000
H	-4.59305200	4.48259000	-0.12748100
H	3.73614400	0.60055400	2.73421500
H	4.72117900	2.59972700	1.72109300
C	3.76689000	3.78318600	0.21379400
H	2.57231700	4.76912100	-1.30057600
C	-2.85922500	-1.27392700	0.91478800
C	-2.13842500	0.49470800	2.42599000
H	4.59266800	4.48327300	0.12742100
C	-4.17270900	-0.72244600	0.94937700
C	-2.61796100	-2.41822200	0.08478000
C	-3.42920700	0.98640200	2.51434400
H	-1.33579800	0.98743400	2.96726500
C	-5.20684100	-1.29010600	0.15191800
C	-4.45795800	0.41235500	1.76094700
H	-1.62137200	-2.83742600	0.04621700
C	-3.61079200	-2.95989000	-0.66746600
H	-3.64216700	1.85200000	3.13485500
C	-4.93407900	-2.41763700	-0.67019200
C	-6.51375800	-0.72561200	0.16316300
C	-5.78515900	0.95164200	1.76400700
H	-3.40129500	-3.81905700	-1.29927300
C	-5.96145000	-2.95250500	-1.45884400
C	-6.76710900	0.41089600	0.99889800
C	-7.50954400	-1.29222800	-0.64100900
H	-5.98535000	1.81763600	2.38937900
H	-5.74965600	-3.81466800	-2.08586100
C	-7.23349900	-2.39399800	-1.44361100
H	-7.76825800	0.83444400	1.00546500
H	-8.50673800	-0.85972400	-0.63053500
H	-8.01809600	-2.82133200	-2.06124400

PyCO in S0 state

Atom	X	Y	Z
O	0.99477900	-1.93894000	-1.18208300
C	1.04888600	-0.82839900	-0.67312200
C	2.35604600	-0.30704800	-0.16460100
C	-0.16160400	0.03967700	-0.56450300
C	3.51030100	-0.85218500	-0.68876500
C	2.44721300	0.66414900	0.86687300

C	-1.43794900	-0.49311500	-0.26191400
C	-0.02851500	1.40465500	-0.84472400
C	4.78404500	-0.43950200	-0.24287900
H	3.42187600	-1.61373700	-1.45886600
C	3.67141300	1.07005300	1.33270900
H	1.53795300	1.06910200	1.29967900
C	-2.55751100	0.39047800	-0.22552000
C	-1.65598100	-1.87684200	0.05203300
H	0.95329100	1.79691600	-1.09276700
C	-1.12047400	2.25555300	-0.84156900
C	4.87008400	0.54346000	0.79031000
C	5.97978300	-0.97452600	-0.78634400
H	3.73667500	1.80326300	2.13246800
C	-3.85210600	-0.10387400	0.10424200
C	-2.39538500	1.77333300	-0.52633100
H	-0.81391200	-2.55543700	0.01089600
C	-2.89169400	-2.34048100	0.37306600
H	-0.99292600	3.30735800	-1.08246300
C	6.14901100	0.95297900	1.24001800
H	5.90691700	-1.72271500	-1.57124000
C	7.20424300	-0.55673200	-0.32916800
C	-4.03348200	-1.48011400	0.40877900
C	-4.97155600	0.77505300	0.13227800
C	-3.53932100	2.63478600	-0.49511700
H	-3.03142600	-3.39262100	0.60775800
H	6.21362000	1.70026300	2.02672100
C	7.28863500	0.41618800	0.69321300
H	8.11460600	-0.97239600	-0.75073300
C	-5.31339400	-1.94765200	0.73259900
C	-4.77067900	2.15849500	-0.17961300
C	-6.23332100	0.26525200	0.46052800
H	-3.39738500	3.68633400	-0.73002900
H	8.26395400	0.73830900	1.04637400
H	-5.44705200	-3.00106900	0.96424300
C	-6.40031300	-1.08249200	0.75799800
H	-5.63025600	2.82344200	-0.15831100
H	-7.08613700	0.93878800	0.47943000
H	-7.38627200	-1.46117700	1.01065100

DFT optimized S1 structure (excited state)

(*R*)-**BiPyCO** in S1 state

Atom	X	Y	Z
C	-6.45999400	-0.83529600	0.34769600
C	-6.69446100	0.28815800	1.20398400
H	-7.70557100	0.68085000	1.27644700
C	-5.13823200	-1.35673300	0.24716600
C	-7.48753500	-1.42994700	-0.39582500
C	-4.07279500	-0.76026600	0.98077500
C	-4.88364300	-2.46673800	-0.60487300
C	-5.68020700	0.85915800	1.90502300

C	-7.22849300	-2.51541000	-1.22539100
H	-8.49502900	-1.02928800	-0.31758200
C	-2.74745500	-1.26928900	0.85966300
C	-4.34206000	0.36484600	1.81194400
C	-3.54688400	-2.96329500	-0.69345100
C	-5.94262800	-3.03035400	-1.33053500
H	-5.86486700	1.72080200	2.54115700
H	-8.03746200	-2.96299800	-1.79585400
C	-1.69826600	-0.57813200	1.51449200
C	-2.52728700	-2.39628200	0.00459500
C	-3.28226100	0.97968500	2.48945600
H	-3.35102700	-3.80795900	-1.34893700
H	-5.74289500	-3.87764800	-1.98142900
C	-0.28304400	-0.99232600	1.39225400
C	-1.98769900	0.52894200	2.32131000
H	-1.52309300	-2.78715700	-0.09055300
H	-3.48055800	1.84721300	3.11175400
O	0.07588600	-2.16720100	1.41473800
C	0.76109900	0.07676300	1.27221300
H	-1.16950000	1.05060800	2.80849700
C	0.63934400	1.10950000	0.34314000
C	1.91246700	-0.05089200	2.08304300
C	1.67352700	2.10354800	0.29477800
C	-0.51554900	1.11520400	-0.59073000
H	1.97513500	-0.90583800	2.74944400
C	2.90948800	0.88672100	2.03627100
C	2.81496300	1.98559400	1.14498300
C	1.62628000	3.17786800	-0.62646100
C	-1.57045200	2.05917000	-0.42372400
C	-0.63906100	0.07888200	-1.56828100
H	3.78728400	0.79718600	2.67105600
C	3.84754200	2.95096900	1.05092800
H	0.76100500	3.25843700	-1.27699200
C	2.64424200	4.09978800	-0.69538800
C	-2.79665800	1.88205600	-1.14515400
C	-1.51005300	3.12818900	0.50897800
C	0.41937200	-0.78432600	-1.98568200
C	-1.89120800	-0.08937000	-2.23791800
H	4.71109800	2.85277400	1.70421600
C	3.76798100	3.98607900	0.15088500
H	2.58319400	4.92102400	-1.40385800
C	-2.92271200	0.77101900	-2.04023200
C	-3.86451300	2.76606800	-0.92849400
H	-0.60748000	3.26773300	1.09503200
C	-2.57356700	3.98965500	0.68843200
O	0.31306200	-1.82212600	-2.68106800
C	1.86695400	-0.41105500	-1.79869800
H	-1.97614500	-0.92542800	-2.92450900
H	4.56698700	4.71981000	0.09055000
H	-3.86873200	0.62491000	-2.55473800

H	-4.79040700	2.59826100	-1.47331900
C	-3.76536700	3.81395500	-0.02846300
H	-2.48756700	4.80158800	1.40592600
C	2.76549100	-1.20855800	-1.02896100
C	2.37083900	0.67733600	-2.52587500
H	-4.60414300	4.48579100	0.12652100
C	4.10602500	-0.77165500	-0.85841200
C	2.34563200	-2.40420900	-0.40326500
C	3.67851700	1.08623400	-2.38018100
H	1.68358400	1.24734500	-3.14062300
C	4.98332100	-1.49143400	-0.01325400
C	4.56896700	0.39333700	-1.52161100
H	1.33751900	-2.75517900	-0.57122000
C	3.20195400	-3.10900900	0.41411300
H	4.02993400	1.97980200	-2.88762100
C	4.52997300	-2.66964900	0.63914000
C	6.30990300	-1.03042100	0.19608100
C	5.89643700	0.83316800	-1.30719400
H	2.84770000	-4.00611900	0.91236100
C	5.41581700	-3.36263500	1.49106800
C	6.74222500	0.14786100	-0.46863900
C	7.15769100	-1.75588900	1.06080300
H	6.23689200	1.73288600	-1.81117200
H	5.06766800	-4.26362400	1.98820000
C	6.71240400	-2.90660200	1.69873300
H	7.75632700	0.50131800	-0.30530000
H	8.17187000	-1.40092400	1.22215200
H	7.37846400	-3.45144800	2.35949900

PyCO in S1 state

Atom	X	Y	Z
O	0.90397400	1.19533100	-2.30997800
C	1.09793000	0.98416600	-1.06867000
C	2.23800900	0.55875100	-0.38088100
C	-0.24967100	1.25537800	-0.49977200
C	3.45268700	0.30471100	-1.06582500
C	2.20872400	0.36207500	1.04167600
C	-1.23752000	0.22125000	-0.46861500
C	-0.62325400	2.57519500	-0.16623800
C	4.59588800	-0.12976900	-0.38320500
H	3.48808500	0.45363100	-2.14063800
C	3.31089800	-0.05928600	1.71668000
H	1.28556800	0.55575300	1.58341200
C	-2.55246400	0.52619400	-0.02942900
C	-0.92372700	-1.11051600	-0.83596300
H	0.13042000	3.35214400	-0.22886500
C	-1.89347900	2.86333800	0.26640400
C	4.54669200	-0.32429200	1.04043600
C	5.82823900	-0.39407300	-1.04530200
H	3.27062800	-0.20303900	2.79391700

C	-3.53303800	-0.49463200	0.03451000
C	-2.89041800	1.85447300	0.34545900
H	0.08261900	-1.32950100	-1.17479300
C	-1.87406000	-2.09902800	-0.77713600
H	-2.15321300	3.87612600	0.56272500
C	5.69289400	-0.76126600	1.71981600
H	5.87931100	-0.24955500	-2.12158300
C	6.93437500	-0.82199800	-0.34729300
C	-3.19835700	-1.82334000	-0.34086300
C	-4.84961200	-0.19243200	0.47606000
C	-4.20825500	2.13465200	0.78072800
H	-1.61892400	-3.11476900	-1.06527800
H	5.63716400	-0.90251500	2.79724900
C	6.87760600	-1.01066400	1.04650500
H	7.86307600	-1.01614200	-0.87772200
C	-4.18879100	-2.82291300	-0.26764700
C	-5.15802400	1.14611100	0.84514400
C	-5.80519600	-1.22376300	0.53180800
H	-4.46020600	3.15231100	1.06516900
H	7.75612400	-1.34799500	1.58773700
H	-3.93250400	-3.83870900	-0.55518000
C	-5.47444900	-2.52329200	0.16371300
H	-6.16452300	1.37691500	1.18275400
H	-6.81280000	-0.99147800	0.86548200
H	-6.22436500	-3.30599300	0.21281600

Copies of NMR spectra

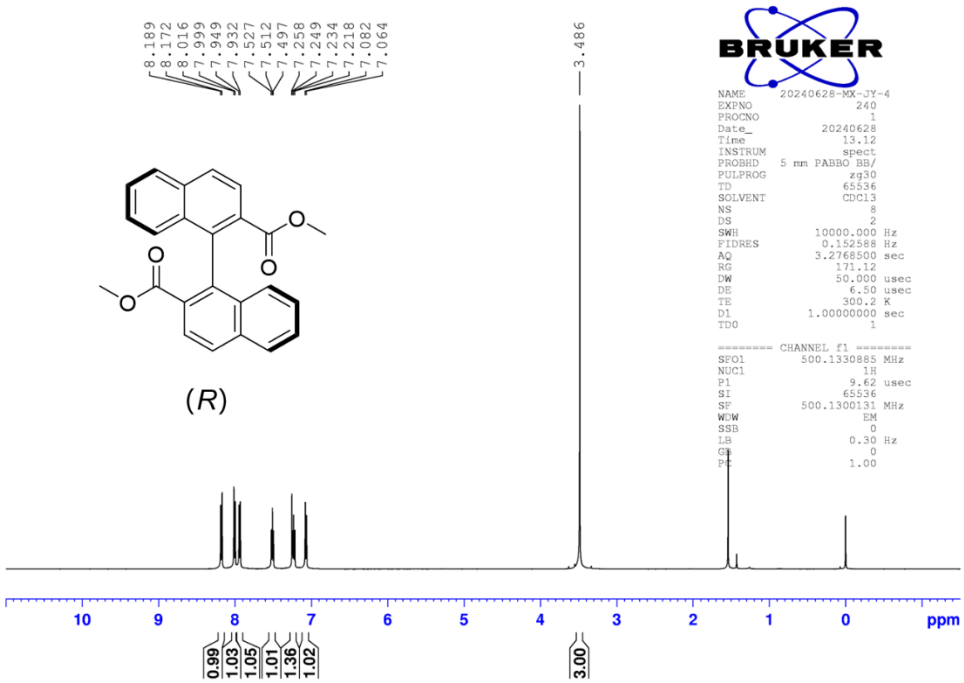

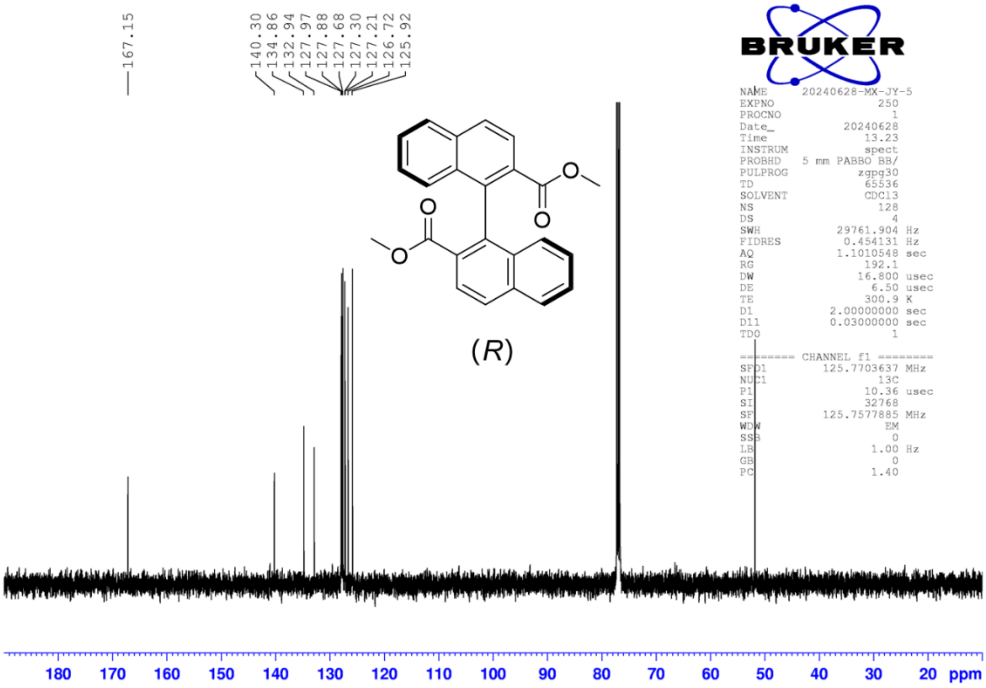

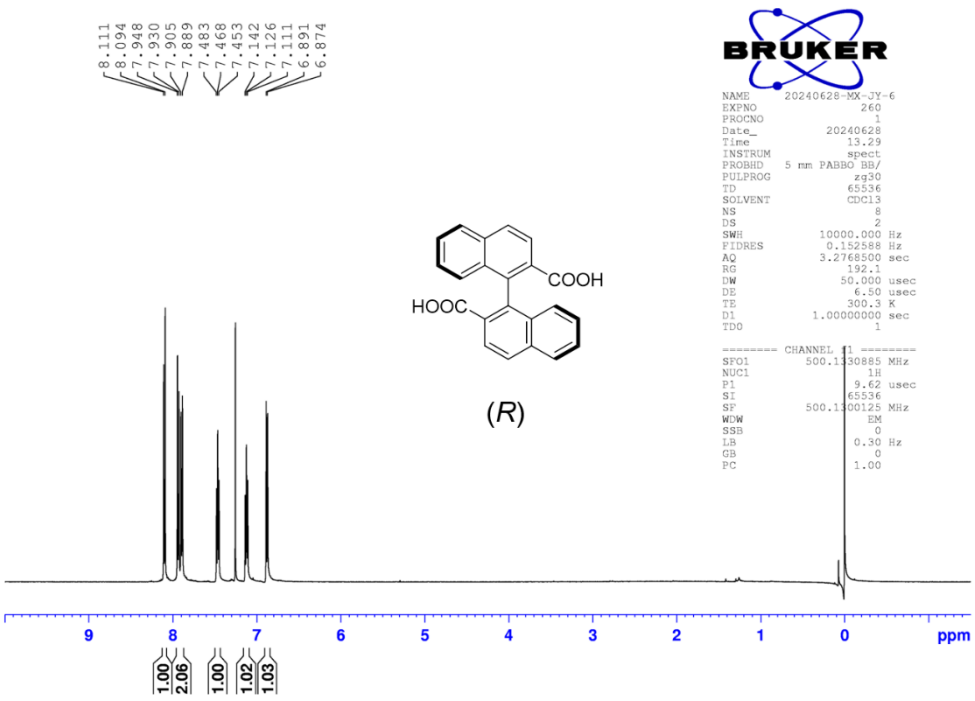
8.111
8.094
7.948
7.930
7.905
7.889
7.483
7.468
7.453
7.142
7.126
7.111
6.891
6.874
COOH
HOOC
(R)
BRUKER
NAME 20240628-MX-JY-6
EXPNO 260
PROCNO 1
Date_ 20240628
Time 13.29
INSTRUM spect
PROBHD 5 mm PABBO BB/
PULPROG zg30
TD 65536
SOLVENT CDCl3
NS 8
DS 2
SWH 10000.000 Hz
FIDRES 0.152588 Hz
AQ 3.2768500 sec
RG 192.1
DW 50.000 usec
DE 6.50 usec
TE 300.3 K
D1 1.00000000 sec
TD0 1
======== CHANNEL f1 ========
SFO1 500.1330885 MHz
NUC1 1H
P1 9.62 usec
SI 65536
SF 500.1300125 MHz
WDW EM
SSB 0
LB 0.30 Hz
GB 0
PC 1.00
9
8
7
6
5
4
3
2
1
0
ppm
1.00
2.06
1.00
1.02
1.03

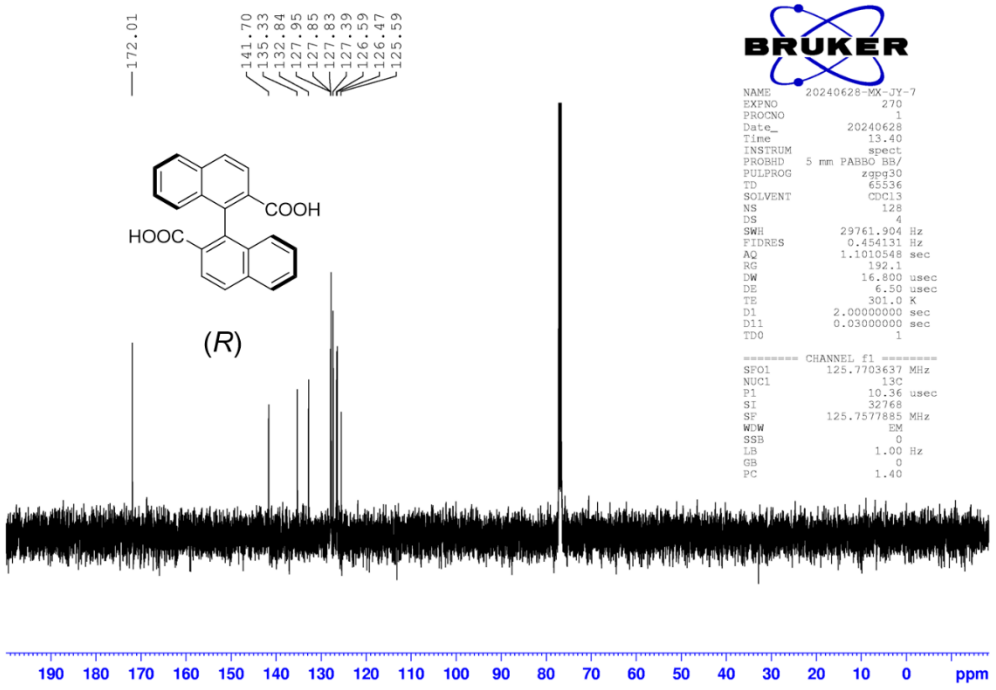
172.01
141.70
135.33
132.84
127.95
127.85
127.83
127.39
126.59
126.47
125.59
COOH
HOOC
(R)
BRUKER
NAME 20240628-MX-JY-7
EXPNO 270
PROCNO 1
Date_ 20240628
Time 13.40
INSTRUM spect
PROBHD 5 mm PABBO BB/
PULPROG zgpg30
TD 65536
SOLVENT CDCl3
NS 128
DS 4
SWH 29761.904 Hz
FIDRES 0.454131 Hz
AQ 1.1010548 sec
RG 192.1
DW 16.800 usec
DE 6.50 usec
TE 301.0 K
D1 2.00000000 sec
D11 0.03000000 sec
TD0 1
======== CHANNEL f1 ========
SFO1 125.7703637 MHz
NUC1 13C
P1 10.36 usec
SI 32768
SF 125.7577885 MHz
WDW EM
SSB 0
LB 1.00 Hz
GB 0
PC 1.40
190
180
170
160
150
140
130
120
110
100
90
80
70
60
50
40
30
20
10
0
ppm

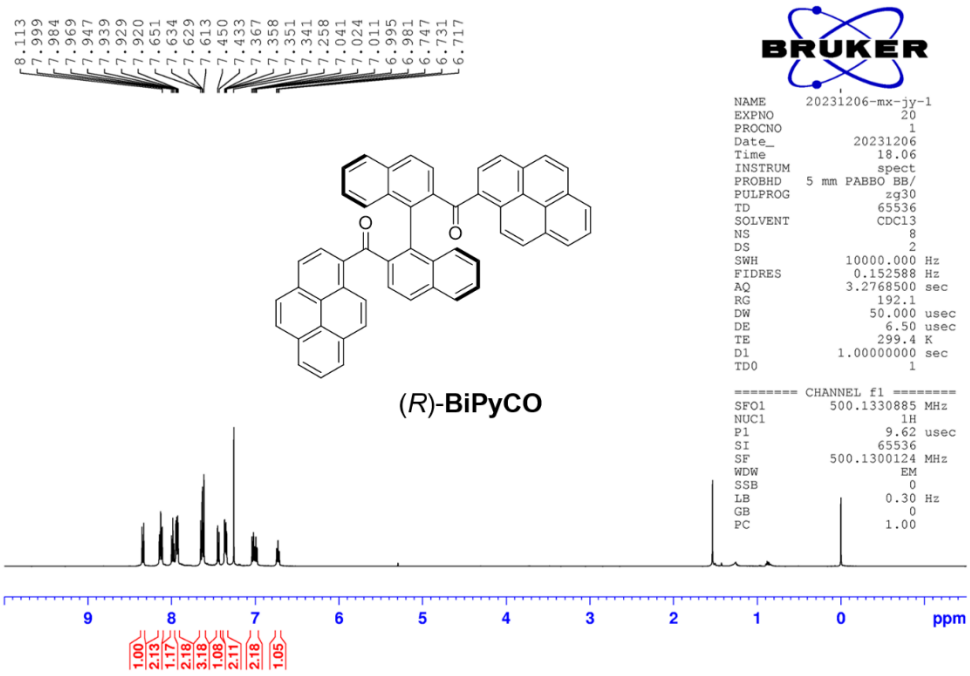
8.113
7.999
7.984
7.969
7.947
7.939
7.929
7.920
7.651
7.634
7.629
7.613
7.450
7.433
7.367
7.358
7.351
7.341
7.258
7.041
7.024
7.011
6.995
6.981
6.747
6.731
6.717
BRUKER
NAME 20231206-mx-jy-1
EXPNO 20
PROCNO 1
Date_ 20231206
Time 18.06
INSTRUM spect
PROBHD 5 mm PABBO BB/
PULPROG zg30
TD 65536
SOLVENT CDC13
NS 8
DS 2
SWH 10000.000 Hz
FIDRES 0.152588 Hz
AQ 3.2768500 sec
RG 192.1
DW 50.000 usec
DE 6.50 usec
TE 299.4 K
D1 1.00000000 sec
TD0 1
======== CHANNEL f1 ========
SFO1 500.1330885 MHz
NUC1 1H
P1 9.62 usec
SI 65536
SF 500.1300124 MHz
WDW EM
SSB 0
LB 0.30 Hz
GB 0
PC 1.00
(R)-BiPyCO
9 8 7 6 5 4 3 2 1 0 ppm
1.00 2.13 1.17 2.18 3.18 1.08 2.11 2.18 1.05

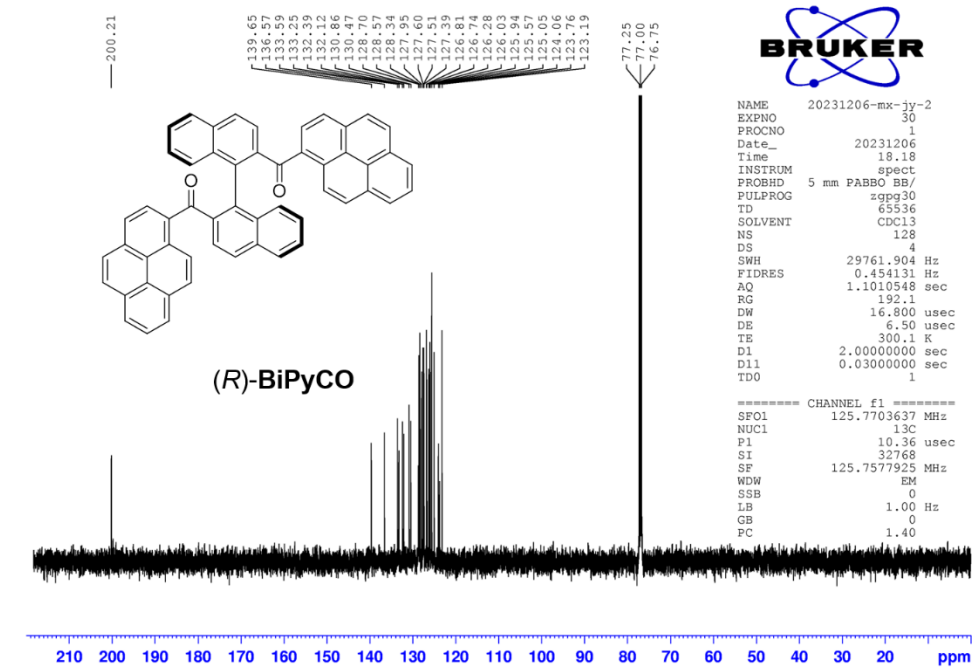
200.21
139.65
136.57
133.59
133.25
132.39
132.12
130.86
130.47
128.70
128.57
128.34
127.95
127.60
127.51
127.39
126.81
126.74
126.28
126.03
125.94
125.57
125.05
124.06
123.76
123.19
77.25
77.00
76.75
BRUKER
NAME 20231206-mx-jy-2
EXPNO 30
PROCNO 1
Date_ 20231206
Time 18.18
INSTRUM spect
PROBHD 5 mm PABBO BB/
PULPROG zgpg30
TD 65536
SOLVENT CDC13
NS 128
DS 4
SWH 29761.904 Hz
FIDRES 0.454131 Hz
AQ 1.1010548 sec
RG 192.1
DW 16.800 usec
DE 6.50 usec
TE 300.1 K
D1 2.00000000 sec
D11 0.03000000 sec
TD0 1
======== CHANNEL f1 ========
SFO1 125.7703637 MHz
NUC1 13C
P1 10.36 usec
SI 32768
SF 125.7577925 MHz
WDW EM
SSB 0
LB 1.00 Hz
GB 0
PC 1.40
(R)-BiPyCO
210 200 190 180 170 160 150 140 130 120 110 100 90 80 70 60 50 40 30 20 ppm

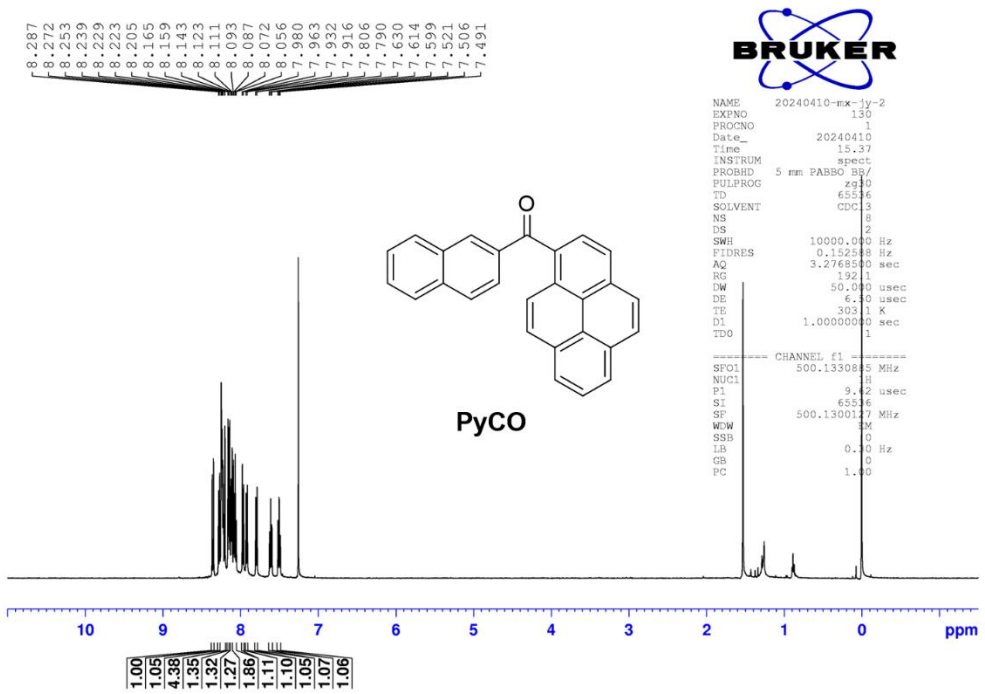
8.287
8.272
8.253
8.239
8.229
8.223
8.205
8.165
8.159
8.143
8.123
8.111
8.093
8.087
8.072
8.056
7.980
7.963
7.932
7.916
7.806
7.790
7.630
7.614
7.599
7.521
7.506
7.491
BRUKER
NAME 20240410-mx-jy-2
EXPNO 130
PROCNO 1
Date_ 20240410
Time 15.37
INSTRUM spect
PROBHD 5 mm PABBO BB/
PULPROG zg30
TD 65536
SOLVENT CDCl3
NS 8
DS 2
SWH 10000.000 Hz
FIDRES 0.152588 Hz
AQ 3.2768500 sec
RG 192.1
DW 50.000 usec
DE 6.50 usec
TE 303.1 K
D1 1.00000000 sec
TD0 1
======== CHANNEL f1 ========
SFO1 500.1330885 MHz
NUC1 1H
P1 9.42 usec
SI 65536
SF 500.1300127 MHz
WDW EM
SSB 0
LB 0.30 Hz
GB 0
PC 1.40
O
PyCO
10 9 8 7 6 5 4 3 2 1 0 ppm
1.00 1.05 4.38 1.35 1.32 1.27 1.86 1.11 1.10 1.05 1.07 1.06

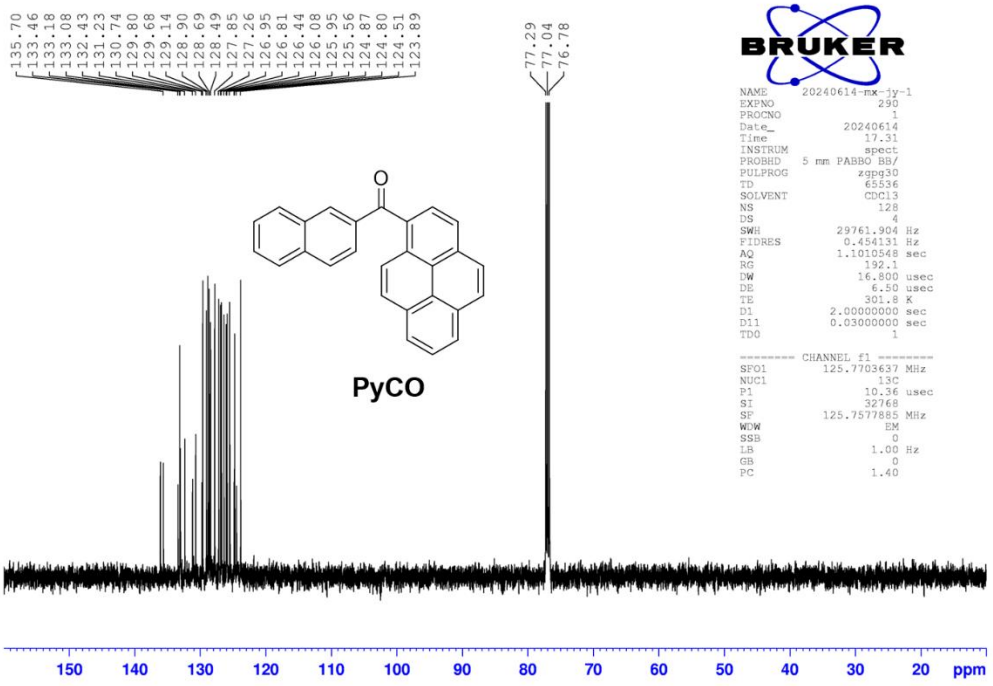
135.70
133.46
133.18
133.08
132.43
131.23
130.74
129.80
129.68
129.14
128.90
128.69
128.49
127.85
127.26
126.95
126.81
126.44
126.08
125.95
125.56
124.87
124.80
124.51
123.89
77.29
77.04
76.78
BRUKER
NAME 20240614-mx-jy-1
EXPNO 290
PROCNO 1
Date_ 20240614
Time 17.31
INSTRUM spect
PROBHD 5 mm PABBO BB/
PULPROG zgpg30
TD 65536
SOLVENT CDCl3
NS 128
DS 4
SWH 29761.904 Hz
FIDRES 0.454131 Hz
AQ 1.1010548 sec
RG 192.1
DW 16.800 usec
DE 6.50 usec
TE 301.8 K
D1 2.00000000 sec
D11 0.03000000 sec
TD0 1
======== CHANNEL f1 ========
SFO1 125.7703637 MHz
NUC1 13C
P1 10.36 usec
SI 32768
SF 125.7577885 MHz
WDW EM
SSB 0
LB 1.00 Hz
GB 0
PC 1.40
O
PyCO
150 140 130 120 110 100 90 80 70 60 50 40 30 20 ppm

Copies of IR spectra

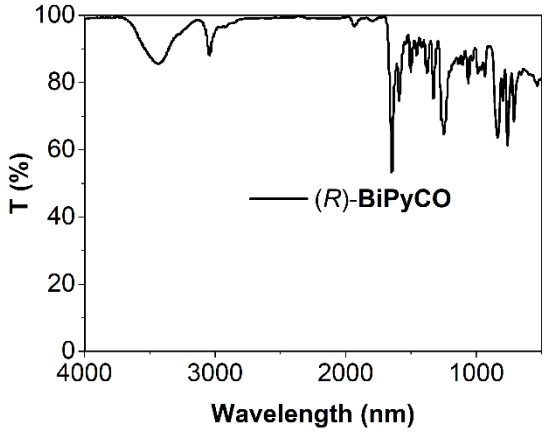

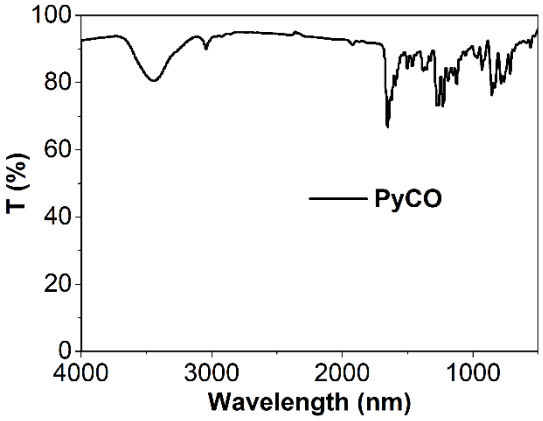

Copies of HRMS